UNIVERSITA' DEGLI STUDI DI NAPOLI

"FEDERICO II"

TESI DI DOTTORATO IN

PATOLOGIA E FISIOPATOLOGIA MOLECOLARE

XXIII° CICLO

Control of PKA stability and signalling by RING ligase praja2

COORDINATORE

Ch.mo Prof. V. E. Avvedimento

CANDIDATO

Dott. Luca Lignitto

SUPERVISORE

Ch.mo Prof. Antonio Feliciello

ANNO ACCADEMICO 2009/2010

ORIGINAL PUBBLICATIONS

1. **Lignitto L.**, Carlucci A., Sepe M., Stefan E., Cuomo O., Nisticò R., Scorziello A., Savoia C., Garbi C., Annunziato L. and Feliciello A. (2010) Control of PKA stability and signalling by RING ligase praja2. Submitted

2. Carlucci A., **Lignitto L.,** Feliciello A. (2008) Control of mitochondria dynamics and oxidative metabolism by cAMP, AKAPs and the proteasome. Trends Cell Biol. 18(12):604-13. Epub 2008 Oct 24.

3. Carlucci A., Gedressi C., **Lignitto L.,** Nezi L., Villa-Moruzzi E., Avvedimento EV., Gottesman M., Garbi C., Feliciello A. (2008) Protein-tyrosine phosphatase PTPD1 regulates focal adhesion kinase autophosphorylation and cell migration. J Biol Chem. 283(16):10919-29. Epub 2008 Jan 26.

INTRODUCTION

1.1 The cAMP-dependent signal transduction pathway

Living cells are exposed to multiple stimuli and the tight regulation of the transduction pathways activated by these signals is crucial to elicit phyisiological responses. Extracellular messengers, such as hormones, neurotransmitters and growth factors, regulate different cellular processes, as cellular differentiation and division, ionic channels activity, gene transcripton and protein translation.

The binding of these molecules to specific cellular receptors elicits cellular responses. Plasma membrane receptors transmit the signals of the specific hydrophilic messengers, generating biophysical modification or increasing intracellular signalling molecules concentration known as second messengers.

The first second messenger identified is the cyclic AMP (cAMP) *(Sutherland et al., 1970)*. cAMP-dependent transduction pathway is mediated by G-coupled receptors that activate the adenylyl cyclase (AC), ubiquitous enzyme converting ATP in cAMP. In mammals, the ubiquitous second messenger cAMP is synthesized by two classes of AC: the G protein responsive transmembrane adenylyl cyclases (tmACs) and the widely distributed, bicarbonate-responsive, soluble adenylyl cyclase (sAC) *(Chen et al., 2000)*. tmACs are characterized by a short NH2-terminal amino-acidic segment and by two cytoplasmic domains (C1 and C2) separated

by two highly hydrophobic transmembrane domains (M1 and M2). C1 and C2 constitute catalytic site of adenylyl cyclase.

cAMP mediates its cellular effects via at least three distinct classes of direct effectors; cAMP-dependent protein kinase (PKA), RAP exchange proteins (EPACs), and cAMP gated ion channels (cNGC). cNGCs and a subset of PKA targets are localized to the plasma membrane, near tmACs, in what appear to be macromolecular signaling complexes comprising the G protein coupled receptor, G protein, tmAC, and PKA and its ultimate substrate *(Zippin et al., 2002)* (**Fig. 1**)

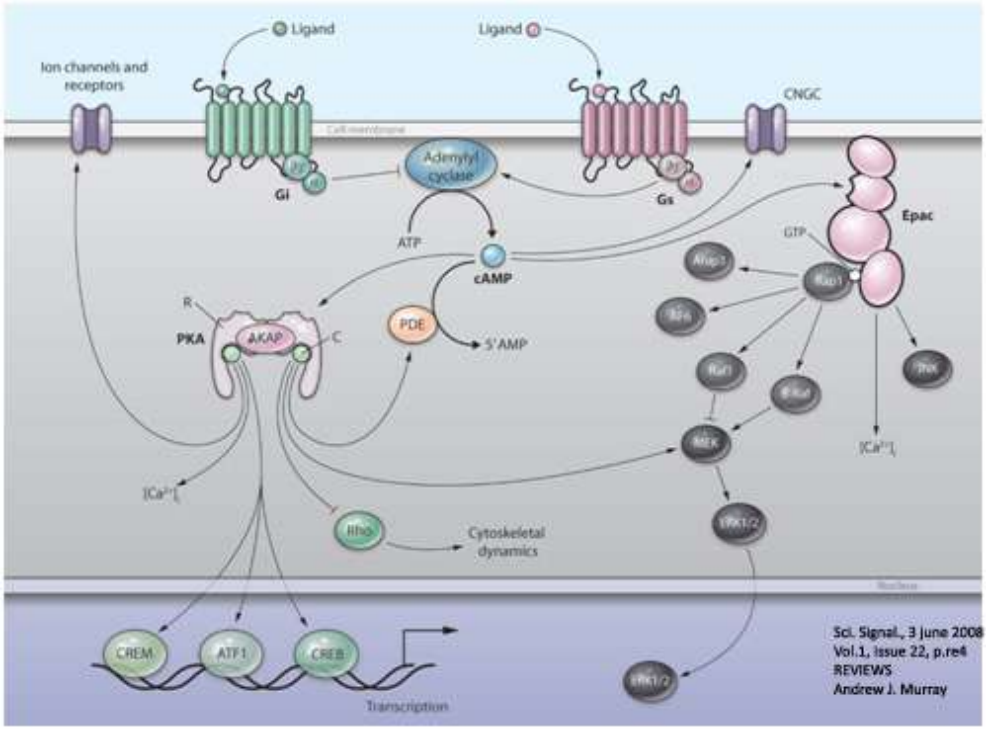

Figure 1. Schematic diagram of cAMP synthesis and downstream effector activation. When an extracellular ligand such as an hormone binds to and activates a seven-transmembrane G-protein-coupled receptor, the signal is passed through the heterotrimeric G protein to adenylyl cyclase. The activated adenylyl cyclase converts ATP into the second messenger cAMP. As the gradient of cAMP concentration diffuses in the cell, various enzymes or effectors are activated.
These include PKA, PDE and EPAC. The interplay of each of these effectors as they interact directly or indirectly with each other and other downstream targets is currently an area of intense study.

1.2 Protein Kinase A (PKA)

Activation of PKA is solely accomplished by the major, diffusible secondary messenger cAMP *(Su et al., 1995).* PKA Holoenzyme is a serine/threonine kinase constitutes by two catalytic subunits (PKAc or C) that are helded in an inactive complex by a dimer of regulatory subunits (Rs). Binding of cAMP to each R subunit relieves the autoinhibitory contact, allowing the C subunits to dissociate *(Wang et al., 1991)* thereby resulting in phosphorylation of local substrates (**fig. 2**). PKA-dependent phosphorylation of nuclear and cytoplasmic substrates controls multiple cell functions, including motility, metabolism, differentiation, synaptic transmission, ion channel activities, growth and coordinate gene transcription *(Edelman et al., 1987; Taylor et al., 1992; Meinkoth et al., 1993; Montminy et al., 1997).*

Two forms of the heterotetrameric PKA holoenzyme exist: type I (RIα and RIβ dimer) and type II (RIIα and RIIβ dimer). Type I PKA is predominantly cytoplasmic, whereas type II PKA associates with specific cellular structures and organelles. Catalytic subunits are encoded from three different genes Cα, Cβ e Cγ, that show common kinetic features and substrate specificity *(Taylor et al., 1992)*. Four genes encode the R subunits R1α, R1β, R2α e R2β *(Taylor et al., 1992),* that confer the different biochemical and

biological characteristics to the PKA isoforms. The R subunit is a modular polypeptide containing an NH_2-terminal dimerization domain, an autophosphorylation site that serves as a principal contact site for the C subunit, and two cAMP binding sites.

The R subunits are differentially distributed in mammalian tissues. RIα and RIIα are ubiquitous, whereas RIIβ is expressed predominantly in endocrine, brain, fat and reproductive tissues *(Edelman et al., 1987; Taylor et al., 1992).* In addition to their distinctive expression and distribution, R subunits differ in their regulation and biochemical properties. The binding affinity to cAMP of RIIβ in vivo is lower relative to RIIα and much lower compared to RIα *(Edelman et al., 1987; Taylor et al., 1992).*

These data imply that holoenzymes containing RI subunits or RII subunits (PKAI and PKAII) decode cAMP signals that differ in duration and intensity: PKAI is activated transiently by weak cAMP signals, whereas PKAII responds to high and persistent cAMP stimulation. Neurons and endocrine cells, which express predominantly PKAII, are adapted to persistent high concentrations of cAMP *(Stein et al., 1987).* The specific biochemical properties of PKA isozymes account, in part, for the differential cellular responses to discrete extracellular signals that activate adenylyl cyclase.

The function(s) in vivo of the specific PKA isoforms in gene expression and cell signaling has been probed using knockout (KO) and transgenic mouse models *(Brandon et al., 1995a).* Ablation of the gene encoding the RIβ tether to deficits in hippocampal long-term depression and depotentiation *(Qi et al., 1996; Brandon et al., 1995b).* Despite a compensatory increase in total PKA activity, in the RIβ KO mice, hippocampal function is impaired, suggesting a unique role for RIβ in synaptic plasticity *(Amieux et al., 1997).* A targeted disruption of the RIIα gene yields viable mice with no physiological abnormalities, implying that PKAI and/or PKAIIβ compensates for the RIIα defect *(Burton et al., 1997, 1999).* Targeted disruption of the mouse RIIβ gene has additional physiological consequences. The mutant mice are lean and have elevated metabolic rates caused by increases in both basal PKA activity and the basal rate of lipolysis *(Cummings et al., 1996; McKnight et al., 1998).* RIIβ KO mice also display defects in neuronal gene expression, learning and behaviour *(Adams et al., 1997; Brandon et al., 1998).*

Living cells developed several regulation system to control the effects of the cAMP/PKA signaling pathway. Termination of cyclic-nucleotide signaling is achieved by PDEs, a superfamily of > 70 different isozymes that degrade cAMP and cyclic GMP (cGMP).

Distinctive tissue distribution, subcellular compartmentalization and differential regulation of these enzymes contribute to the establishment of local cAMP gradients by limiting the diffusion of cAMP that is generated by adenylyl cyclases *(Houslay et al., 2003).* The type-4 PDEs are a family of > 16 distinct isoforms that have a conserved catalytic core. Divergence within the N-terminal region of PDE4 isoforms enables association with various proteins and, therefore, differential subcellular targeting and regulation. Importantly, the PDE4D3 isozyme has been shown to be part of signaling complexes that target PKA.

The action of PKA, as with many other serine/threonine kinases, is counterbalanced by specific protein phosphatases. In some cases, it has been demonstrated that phosphatases belonging to the PP1 and PP2A families are responsible for dephosphorylation of PKA substrates. In turn, PKA can control phosphatase activity by phosphorylation of specific PP1 inhibitors, such as I-1 and DARPP32 *(Fimia et al., 2000)*.

PKA is targeted at specific intracellular microdomains through interactions with A-Kinase-Anchor-Proteins (AKAPs). AKAP forms a local transduction unit, which includes different signalling/metabolic enzymes, receptors, ion channels, adaptor molecules and mRNAs. In this context, the spatio-temporal kinase

activation provides a control mechanism to direct, integrate and locally attenuate the cAMP cascade.

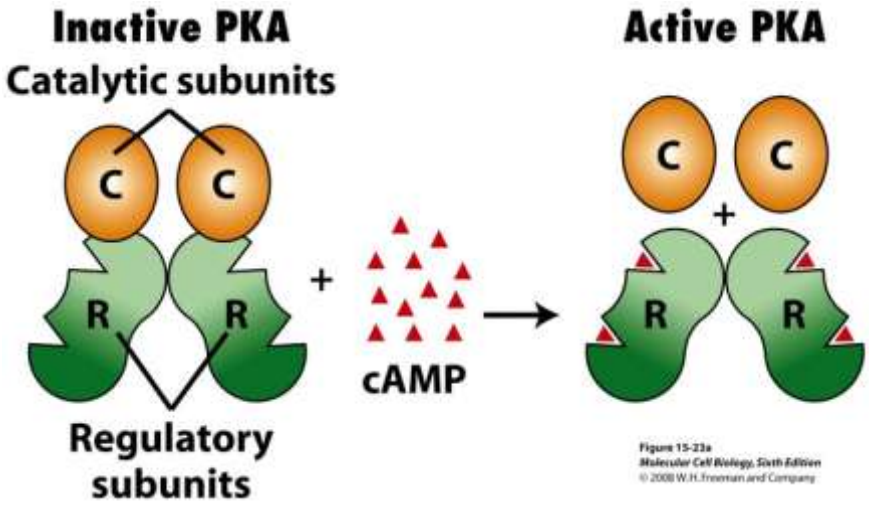

Figure 2. PKA molecular structure and activation mechanism.

1.3 AKAP proteins

Subcellular targeting through association with anchoring proteins has emerged as an important mechanism by which the cells localize signalling enzymes to sites where they can be accessed optimally by activators and, in turn, interact with particular substrates. The PKA is concentrated in particulate membranes and cellular organelles through interaction with a family of non-enzymatic scaffold proteins: A Kinase Anchor Proteins (AKAPs) *(Rubin, 1994; Edwards & Scott, 2000; Dodge & Scott, 2000).*

AKAPs are a group (> 50 proteins) functionally, rather then structurally, related proteins and each contains a common RII-binding site formed by 14–18 amino acid amphipathic aligned along one face of the helix and charged residues and the other side, that bind amino termini of PKA-RII dimer *(Carr et al., 1991; Newlon et al., 1999)* (**Fig. 3**). The first 30 amino acid residues of RII participate in AKAP binding, as shown by site-directed mutagenesis, biochemical analysis and solid-phase binding assays *(Li & Rubin, 1995; Hausken et al., 1994, 1996).* These residues also promote dimerization of RII subunits, which is a prerequisite for binding to AKAP. Although most AKAPs that have been characterized to bind to RII subunits with high affinity, several AKAPs have been reported to interact specifically with RI.

RII subunits bind to AKAPs with nanomolar affinity, by contrast, RI subunits bind to AKAPs with only micromolar affinity. However D-AKAP1 and D-AKAP2 are examples of dual-specificity AKAPs that can anchor both types of R subunit *(Huang et al., 1997; Wang et al., 2001).*

Structural data indicate that there is a single region of multiple contact sites between the RII subunit dimer and the AKAP, which presumably for the high-affinity interaction. Functionally, this suggests that the AKAP–PKA complex is likely to be a constitutive interaction in cells and not subject to regulation. However, the distribution of the PKA holoenzyme can be altered upon induction of AKAP expression. Thereby, regulation of PKA localization might be a function of AKAP targeting.

Each AKAP also contains a subcellular targeting domain that restricts its localization within the cell. A combination of subcellular-fractionation and immunohistochemical studies have identified AKAPs in association with a variety of cellular compartments, including centrosomes, dendrites, endoplasmic reticulum, mitochondria, nuclear membrane, plasma membrane and vesicles. Although AKAPs have been defined on the basis of their interaction with PKA, an additional feature of many of these molecules is their ability to bind to other signalling enzymes, such

as protein phosphatases and kinases. AKAPs form a multiproteic complex with the presence of signal transduction and signal termination enzymes in the same network. This creates focal points of enzyme activity where the bidirectional regulation of signaling events can be controlled and the phosphorylation status of target substrates is precisely regulated. *(Feliciello et al., 2001)*

AKAP forms a ``transduceosome'' by acting as an autonomous multivalent scaffold that assembles and integrates signals derived from multiple pathways. The transduceosome amplifies cAMP and other signals locally and, by stabilizing and reducing the basal activity of PKA, it also exerts long-distance effects. The AKAP transduceosome thus optimizes the amplitude and the signal/noise ratio of cAMP-PKA stimuli travelling from the membrane to the nucleus and other subcellular compartments *(Feliciello et al., 2001).*

Importantly, Besides kinase and phosphatase, recent reports have demonstrated that phosphodiesterases, the enzymes that catalyze cAMP metabolism, are present in complex with AKAP and PKA. These findings add a novel twist to PKA regulation, as they indicate that an anchored pool of phosphodiesterase may tightly control local cAMP levels.

AKAPs, anchoring the PKA in close proximity of the substrates, optimize the PKA-dependent phosphorylation of a plethora of cellular substrates.

Cells that express high levels of membrane-bound PKA are more sensitive the cAMP increase *(Feliciello et al., 1998, Feliciello et al., 2000)*. This might be explained by the fact that membrane-bound PKA is more stable than the cytosolic enzyme *(Feliciello et al., 1996)*. PKA levels are higher in cells containing a high fraction of membrane-bound PKA, and the effects of PKA activation are more readily transmitted from the point of cAMP generation at the cell membrane *(Lester et al., 1997; Paolillo et al., 1999; Cassano et al. 1999).*

This interaction between AKAPs and cAMP, defines a positive regulatory loop in which the second messenger stimulates AKAP expression that in turn enhances cAMP dependent signaling pathway. In this way anchor proteins are involved in a potent regulatory mechanism that, coordinating and integrating several cellular processes, controls the specificity of signal transduction.

In higher eukaryotes, essential functions such as neurite outgrowth and morphogenesis, synaptic transmission, hormones production and release, require tightly regulated response to PKA stimulation.

The cAMP/PKA pathway plays a crucial role in synaptic plasticity in a wide variety of species. Pharmacological or genetic inhibition of PKA severely affects the induction of hippocampal long-term potentiation (LTP) and inhibits synaptic plasticity and long-lasting memory *(Huang et al., 1994).* In Aplysia sensory neurons, the switch from short-term (STF) to long-term facilitation (LTF) is essential for initiating stable long-term memory. Ubiquitin-dependent proteolysis of R subunits sustains nuclear PKAc signaling and promotes transition from STF to LTF, thereby contributing to synaptic strengthening *(Chain et al., 1999a, 1995 1999b; Hedge et al., 1997).* In mammals, proteolysis of R subunits has been linked mechanistically to differentiation and co-ordinated progression through cell cycle *(Feliciello et al., 2000).* However, the identity of the E3 ubiquitn ligase controlling PKA stability in eukaryotes is so far unknown.

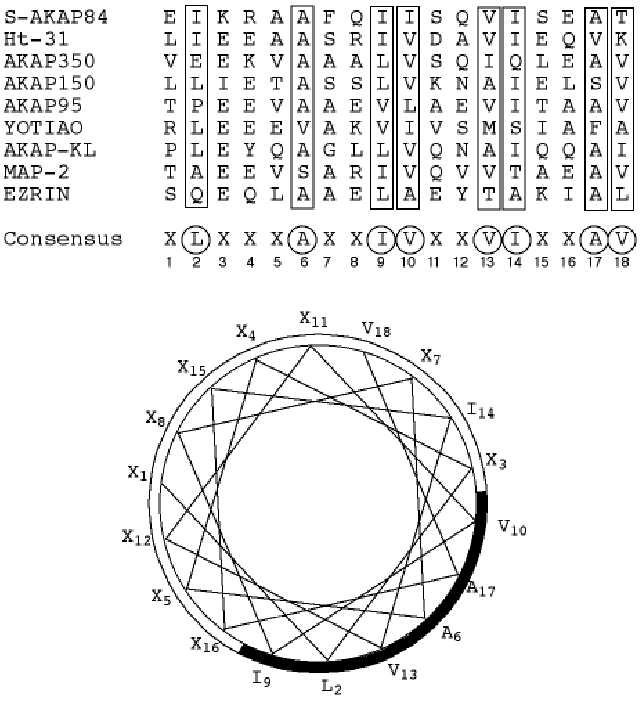

Figure 3. Consensus sequence of AKAP-RII-binding domains.

Consensus sequence derived from the alignment of the primary sequences of several AKAPs (upper). The amphipathic helical wheel and the residues forming it are depicted as a thick line (lower).

1.4 praja2

Regulation of protein stability is largely mediated by ubiquitin ligases, which mark their substrates for efficient proteasome-dependent degradation *(Hershko et al., 1998).* The conjugation of ubiquitin moieties to substrates requires coordinated action of the ubiquitin activating enzyme (E1), the ubiquitin conjugating enzyme E2 and the E3 ligase, which associates with the substrate and thereby determines the specificity in degradation of various substrates *(Ciechanover, 1998)* **(Fig. 4).**

The RING finger ubiquitin E3 ligases contain a characteristic cysteine-rich zinc binding domain defined by a pattern of conserved cysteine and histidine residues. These ligases efficiently catalyze poly-ubiquitination of given substrates *(Joazeiro et al., 2000)*. Characteristic of RING finger ubiquitin E3 ligases is the ability to mediate degradation of their substrates, as well as their own availability, by promoting their own ubiquitination-dependent degradation *(Lorick et al., 1999)*.

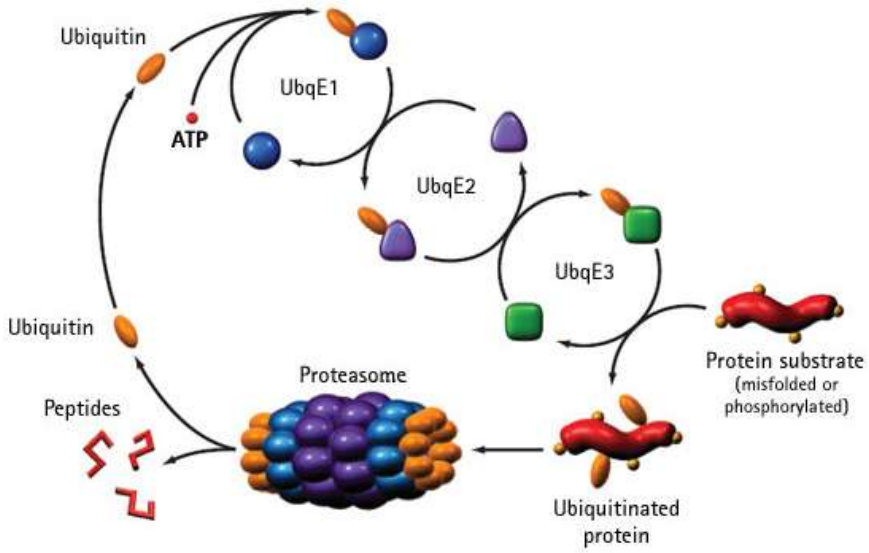

Figure 4. Schematic representation of proteasomal degradation.

praja2 (PJA2) could be categorized into Ring H2 finger E3 ubiquitin ligase subfamily. Structural studies and sequence analysis, in fact, revealed that this protein contains at COOH-terminal end (aa 629-678) a characteristic sequence domain known as the RING-H2-finger motif *(Freemont, 1993).* [the RING-H2-finger motif is closely related to the RING-finger motif, and Cys4 in the RING-finger motif is replaced by His *(Freemont, 1993)*] (**Fig. 5)**.

praja E3 ligase family recognises two members that share high sequence homology.

Figure 5. Sequence alignment of the RING-H2-finger family.
The metal binding ligands, which are absolutely conserved between the family members, are indicated by asterisks, as are the positions of conserved hydrophobic residues indicated by #. The numbering (1-6 and 1-2) below each conserved Cys and His refers to the potential metal binding ligands C1-C6 and H1-H2, respectively. The numbering in parentheses refers to the protein sequence.

praja2 gene is localized on the long arm of human chromosome 5 (5q21). 5.2 Kbp transcript encodes a 708 amino-acidic residues protein, with an estimate weight of 78 Kda *(Nakayama et al., 1995).*

praja1 (PJA1) gene mapped on human chromosome X. Northern blot analysis identify a 2.7 Kbp ribonucleotide transcript, coding a 643 amino-acids protein, with an estimate weight of 71 kda *(Ping et al., 2002)*.

Furthermore, different splice variants have been recognized. praja1 shows high sequence homology with praja2 (52.3% of identity). Besides the COOH terminal domain contains an highly conserved RING H2 Finger domain. (**Fig. 6)**.

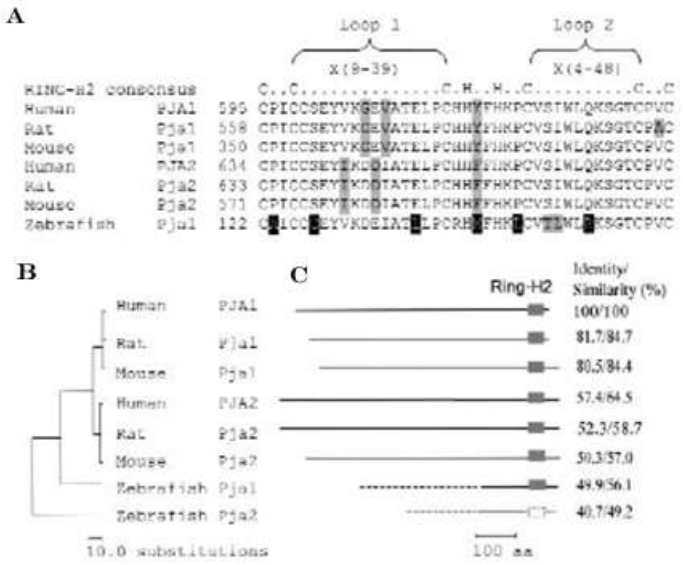

Figure 6. Human praja2 and its orthologous and homologous proteins in different species.

(**A**) Multiple sequence alignment of RING-H2 regions from praja2 and praja1 sequences across various species. Loops and predicted coordination sites are indicated above. Similar amino acids are in gray and different amino acids are in black boxes. The RING-H2 consensus sequence is $CX_2CX(9–39)CX(1–3)HX(2–3)HX_2CX(4–48)CX_2C$. (**B**) A phylogenetic tree of praja1 and homologous sequences generated from sequence alignments. The scale bar beneath the tree represents 10 substitutions per 100 residues. (**C**) Representation of praja1 and praja2 proteins with RING-H2 motifs. Dashed lines represent incomplete sequences. A dashed open box represents an incomplete sequence of RING-H2 motif. The percent identity/similarity for each of these eight proteins compared with the human praja1 is shown on the right side. The names of each of these proteins are respectively listed in (B).

Interestingly praja1 expression is pronounced and show learning-specific induction in the basolateral complex of the amygdala during formation of fear memory *(Stork et al., 2001).* These findings support an important role in mice for praja1 in neuronal

plasticity that is the basis for learning and memory *(Ping et al., 2002).*

Moreover praja1 gene mapped into human chromosome Xq12, where several X-linked mental retardation (MRX) disorders have been associated *(Wilson et al., 1991; Siderius et al., 1999).*

Neurodap1 (Ndap1, Neurodegeneration associated protein 1) gene, the praja2 rat ortolog, is localized on the chromosome 9 (9q37). 4.8 Kbp ribonucleotide transcript encodes a 707 amino-acidic residues RING H2 Finger protein (with an estimate weight of 78 Kda), that shows the 88% identity with praja2.

Although the molecular mass of Ndap1 and praja2 is estimated to be about 140 kDa by SDS-polyacrylamide electrophoresis, this value is larger than the expected one deduced from the primary structure (about 80 kDa). This discrepancy between the expected and observed molecular masses might be explained by anomaly of protein migration rates on SDS-polyacrylamide gel *(Ohara and Teraoka, 1987).*

RNA blotting analysis in rat revealed that the brain is the most abundant in Ndap1 mRNA among different tissues. Lower expression levels were found into the spleen, lung, liver, kidney, testis, heart, thyroid and skeletal muscle *(Nakayama et al., 1995)*.

By in situ hybridization the signals for mRNA of Ndap1 were observed exclusively on the perikaryal cytoplasm of neuronal cells, especially on that of large-sized nerve cells, such as pyramidal cells in the cerebral cortex or hippocampus, Purkinje cells and those in the brainstem *(Nakayama et al., 1995)*.

Strong hybridization signals for mRNA of Ndap1 were observed on the large nerve cells of the facial nuclei, instead weaker signals were detected on the granule cells of the hippocampal dentate gyrus.

Immunoistochemistry analysis on 1 μM thick sections revealed that Ndap1 was distributed in the cytoplasm forming a characteristic punctate pattern and that the distribution of the protein in the brain cells was identical to that of the mRNA-positive cells observed by in situ hybridization *(Nakayama et al., 1995)*. Immunoelectron microscopy analysis shows that Ndap1 is expecially concentrated around the cytoplasmic surface of endoplasmic reticulum (ER), Golgi apparatus, some tiny vesicles and cell membrane.

In particular, the immunoreactivity of Ndap1 was often observed in the postsynaptic density (PSD) region of axosomatic synapses: 35% of the PSDs of axosomatic synapses is decorated with Ndap1 in the nerve cells of the facial nucleus, whereas most of the PSDs

of axosomatic synapses in the cerebral cortex are associated with Ndap1. This observation indicates that the association of Ndap1 to PSD significantly depends on types of PSD *(Nakayama et al., 1995)*.

Following axotomy, axonal degeneration and neuronal cell death correlate with strong down-regulation of Ndap1 expression levels *(Nakayama et al., 1995)*. Thus, regulating synaptic communication and plasticity, PSDs formation and nerve cells viability, praja family proteins may play a crucial role in neuronal activity and development *(Nakayama et al., 1995)*.

Ubiquitin-dependent protein degradation is involved in many cellular processes regulation, such as cell cycle progression and signal transduction, transcription and DNA repair, apoptosis and vescicular transport.

Interestingly, several RING finger genes have been found that are mutated in human diseases *(Mattson et al., 2001; Kitada et al., 1998).* For instance, the parkin gene was found to be mutated in autosomal recessive familial juvenile Parkinsonism *(Kitada et al., 1998).* Many RING finger proteins have unknow functions or unrelated to the ubiquitination in evident manner.

Structural data and sequence analysis identified in praja2 COOH terminal domain (aa 583-600) a particular motif, highly conserved

among all the praja family members, encoding an α amphipathic helix. This domain is characteristic of AKAPs family proteins, and is known to be foundamental for PKA anchoring (**Fig. 3**).

AIM OF THE STUDY

The relative abundance of R and PKAc subunits contributes to the strength and duration of cAMP signalling. Increased PKAc activity sustains downstream cAMP signalling impacting on different aspects of cellular behaviour *(Davis et al., 1998; Amieux et al., 2002).* Several studies reaveal that ubiquitin-dependent proteolysis of R subunits, sustaining nuclear PKAc signaling, promotes transition from STF to LTF, thereby contributing to synaptic strengthening and memory formation *(Chain et al., 1999a, 1995 1999b; Hedge et al., 1997).* In mammals, proteolysis of R subunits has been linked mechanistically to differentiation and co-ordinated progression through cell cycle *(Feliciello et al., 2000).* However, the identity of the E3 ubiquitn ligase controlling PKA stability in eukaryotes is so far unknown.

Using a yeast two hybrid screening, we found praja2 as novel interactor of PKA regulatory subunits.

praja2 is a member of RING H2 Finger E3 ubiquitin ligase. Furthermore computational analysis revealed an amphipathic α−helix (prototypical AKAPs R-binding domain) in COOH terminal of the protein.

These data prompted us to investigate if E3 ligase praja2 may anchor PKA and regulate the stability of R subunits by ubiquitin-

proteasome pathway. So the principal aim of my work has been to identify the role of praja2 as a new important regulator of PKA stability and activity, and of the cAMP signalling transmission pathway .

Therefore, I focused my work at:

- Verify the existence of PKA-praja2 complex.
- Demonstrate that E3 ligase praja2 ubiquitinates and regulates R subunits stability.
- Defining the biological relevance of praja2 activity in regulating cAMP signalling transmission.

RESULTS

2.1 praja2 and RII form a stable complex

To identify novel PKA interacting proteins a rat cDNA library was screened by yeast two hybrid using mouse full-length RIIα as bait. One positive clone (RBP33) of the screen encoded an open reading frame of 178-amino acids corresponding to residues 531-708 of rat praja2 (also named Neurodap1*)(Yu et al., 2002; Nakayama et al., 1995)*(**Fig. 7A**). praja2 belongs to the family of RING proteins that function as E3 ubiquitin ligases that target cellular substrates for proteasomal degradation *(Yu et al., 2002)*.

Moreover we investigated whether endogenous praja2 and R subunits interact in cell extracts. Lysates from HEK293 cells were immunoprecipitated with anti-RIIα/β or non-immune IgG. Precipitates were immunoblotted with anti-RIIα/β or anti-praja2 polyclonal antibody. As shown we detected an endogenous praja2-RII complex (**fig. 7B**).

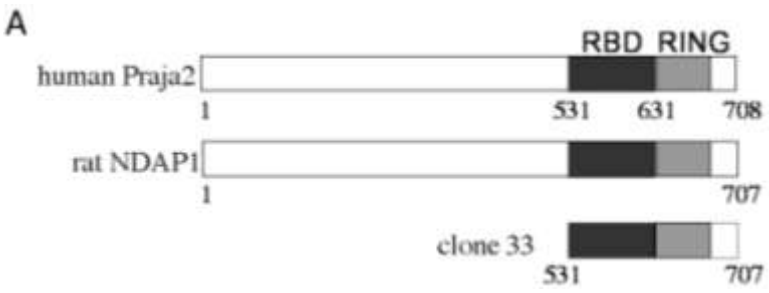

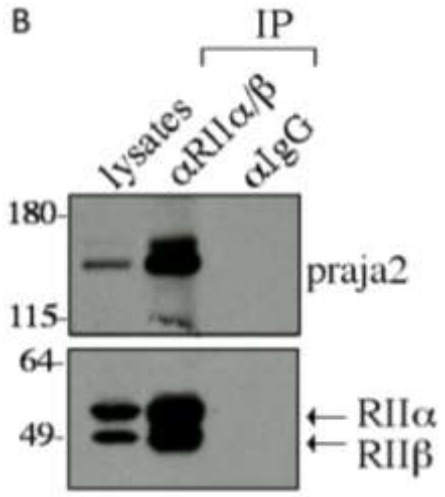

Figure 7. praja2 binds PKA R subunits. (**A**) Schematic representation of human praja2 and its rat homolog neurodap1 (NDAP1, accession # NP_620251). Cysteine-rich region (RING) and the C-terminal rat clone 33 isolated by yeast two-hybrid are shown. RBD, R-binding domain. Sequence of the RING-H2 domain of human praja2 along with the consensus sequence (boxed residues) are shown. Cysteines 634 and 671 substituted with alanines are indicated. (**B**) Lysates (2mg) from HEK293 cells were immunoprecipitated with anti-RIIα/β or non-immune IgG. Precipitates were immunoblotted with anti-RIIα/β or anti-praja2 polyclonal antibody.

2.2 Mapping the PKA binding domain on praja2

To determine if praja2 ligase activity is required for RII binding, HEK293 cells were transiently transfected with flag tagged praja2 and flag tagged praja2 inactive mutant carrying an alanine substitution of two critical residues within the RING domain (cys634 and cys671) (praja2rm). Since praja2 promotes degradation of R subunits (see below), cells were treated for 15 hours with the proteasome inhibitor MG132 and lysates were immunoprecipitated with anti RIIα/β antibody. praja2 ligase activity is unnecessary for RII binding since praja2rm binds RII, even more avidly than wild type praja2 (**Fig. 8A**). As control, we used praja2 deleted of the residues 531-708 (see below).

Furthermore, praja2 also binds RIα subunits (**Fig. 8B**). To identify the domain of the protein that mediates binding with R, we generated a series of praja2 deletion mutants. Flag-tagged praja2 mutants were co-expressed with HA-RIα in HEK293 cells treated for 15 hours with MG132. Lysates were immunoprecipitated with anti-RIα antibody. We found that residues 531 to 631 of praja2 are required for optimal binding to RIα (**Fig. 8B**).

PKAc was also present in the praja2 complex (**Fig. 8C**), presumably through interaction with R subunit, since deletion of the R binding domain of praja2 (residues 531-631) drastically reduced the

amount of flag-praja2 recovered in the PKAc immunoprecipitates (**Fig. 8C**).

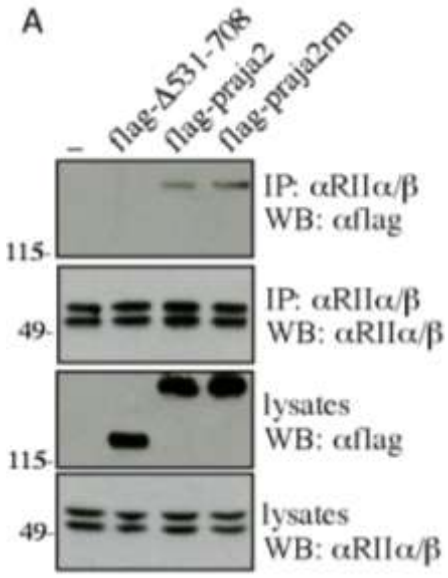

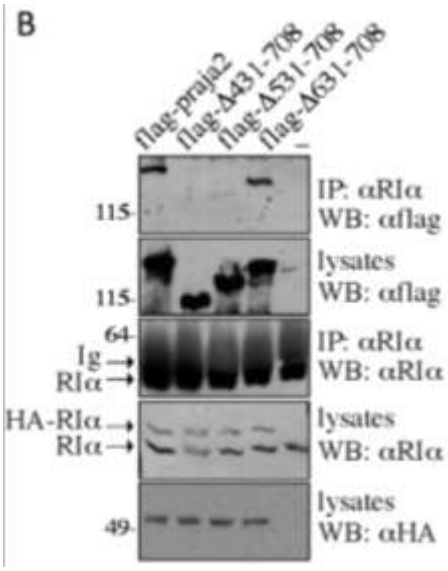

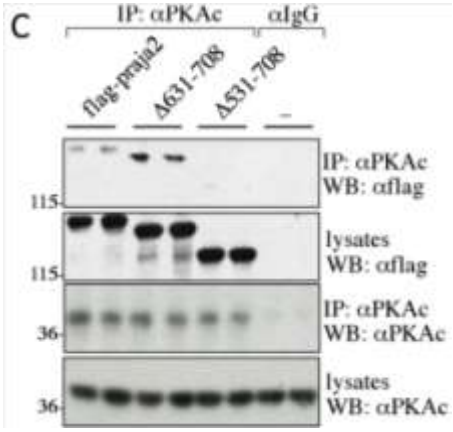

Figure 8. praja2 531-631 residues mediate the binding to R subunits. (**A**) praja2-flag, its RING mutant (Cys634,671Ala) or deletion mutant (Δ531-708) were transiently transfected in HEK293 cells. Lysates were immunoprecipitated with anti-RIIα/β and immunoblotted with anti-flag and anti-RIIα/β antibodies (lower gels). (**B**) praja2-flag or its deletion mutants (Δ631-708, Δ531-708 and Δ431-708) were expressed, along with HA-tagged RIα, in HEK293 cells. Lysates were subjected to co-immunoprecipitation with anti-RIα and immunoblotted with anti-RIα, anti-HA and anti-flag antibodies. (**C**) Lysates from praja2-flag (wild type and mutants) transfected cells were immunoprecipitates with anti-PKAc antibody and immunoblotted with anti-PKAc and anti-flag antibodies.

2.3 praja2 directly interact with Rs

praja2 directly interacts with R subunits. Thus, a fusion protein carrying the full-length praja2 appended to the C-terminus of glutathione S-transferase polypeptide (GST) pulled down *in vitro* translated ^{35}S-labeled R subunits (**Fig. 9A**), as well as endogenously expressed RIIα/β and RIα subunits (**Fig. 9A**). Residues 531-631 of praja2 are necessary and sufficient to bind R subunits *in vitro* (**Fig. 9B**).

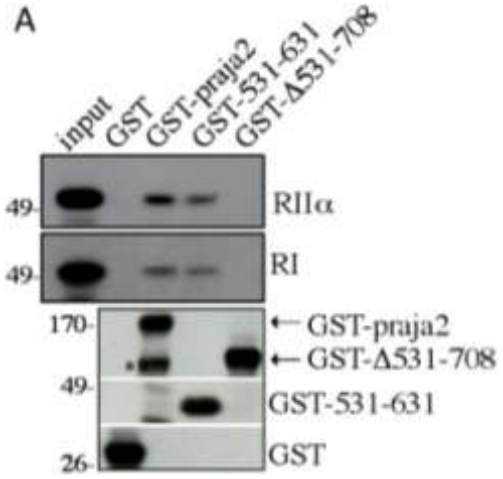

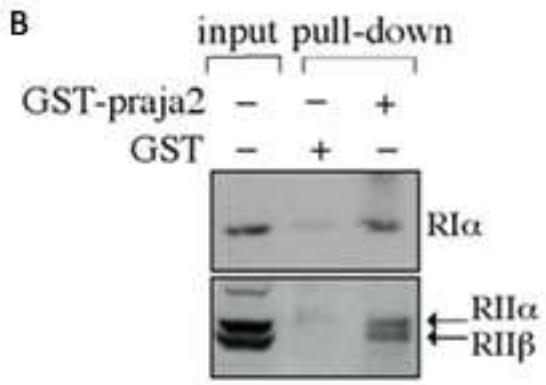

Figure 9. praja2 directly interacts with R subunits *in vitro*. (**A**) *In vitro* translated, ^{35}S-labeled RIIα/β and RIα subunits were subjected to pull-down assays with purified GST-praja2, GST-Δ531-708 and GST-531-631 fusions. (**B**) Cell lysates (2 mg) were incubated with purified GST-praja2 or GST polypeptide. GST beads-bound and input (5%) fractions were immunoblotted (or WB as shown in figure) with anti-RIα and anti-RIIα/β.

2.4 praja2 is an A-Kinase Anchor Protein

Computational sequence analysis of praja2 predicted the presence of a highly conserved amphipathic α–helical wheel (prototypical AKAPs R-binding domain) at position 583-600 that may coordinate the binding to R subunits *(Beene et al., 2007; Tasken et al., 2004)*. As predicted, a synthetic peptide spanning this domain efficiently competed in overlay assay RIIα/β binding to two prototypic PKA binding proteins, MAP2c *(Rubino et al., 1989)* and AKAP75 *(Bregman et al., 1991)* (**Fig. 10A**). As control, we used a peptide carrying proline residues within the amphipathic helix.

The AKAP binding domain resides at the N-terminus of R subunits (residues 1-30) *(Feliciello et al., 2001).* To test if praja2 binds to the AKAP-binding domain of an R subunit, we performed GST-praja2 pull-down assays in the presence of a molar excess of a polypeptide ($AKAP121_{200-450}$) containing the R binding domain of mitochondrial AKAP121. $AKAP121_{200-450}$ competed the RII binding to praja2 (**Fig. 10B**), indicating that simultaneous RII binding to AKAP121 and praja2 is impossible.

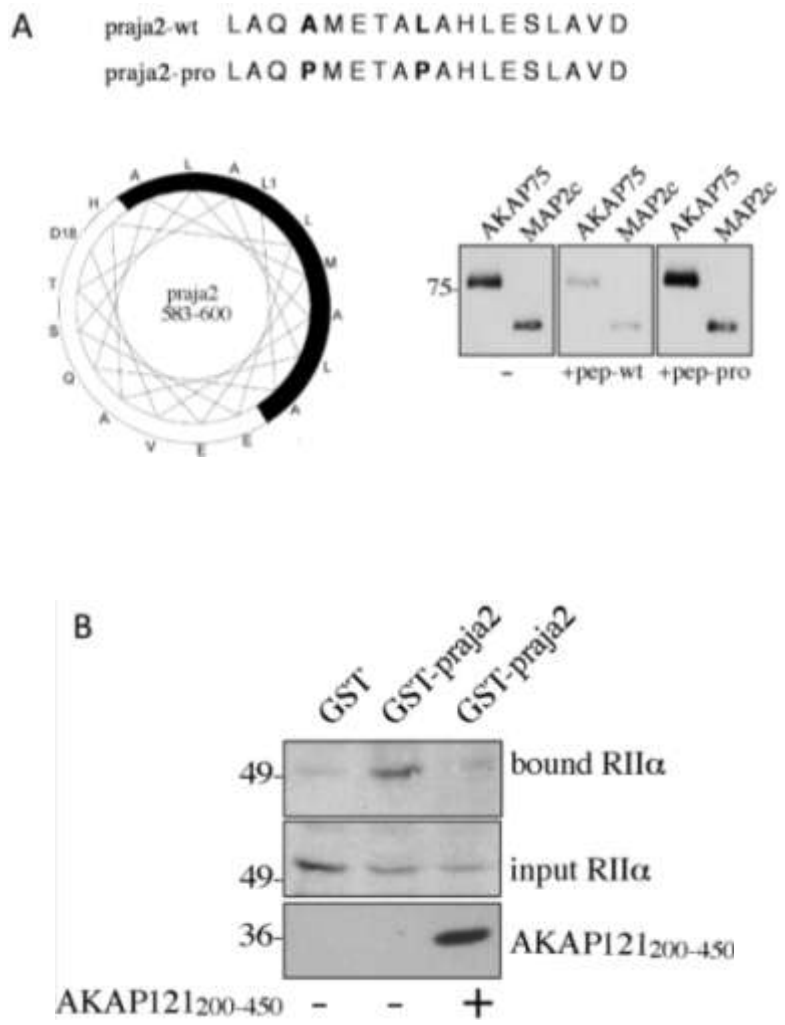

Figure 10. praja2 amphipathic α–helical wheel co-ordinate binding to RII. (**A**) Primary sequence of the residues 583-600 of human praja2 along with helical wheel representation. Hydrophobic face in bold. 1 μg of recombinant MAP2c and AKAP75 were loaded on SDS-PAGE, transfered to nylon membrane and overlayed with purified RIIβ (200ng/ml), in presence or absence of praja2 peptide (1μM), either wt (pep-wt) or proline mutant (pep-pro). After extensive washes in binding buffer, bound RIIβ was revealed by immunoblot analysis with anti-RIIβ antibody. (**B**) HEK293 lysates were subjected to pull down assay using GST-praja2. Where indicated, molar excess (20γ) of recombinant AKAP121 poliptide ($AKAP121_{200-450}$) was added to the lysate. Bound and input fractions were immunoblotted with the indicated antibodies.

2.5 praja2 distribution in rat brain

We next performed colocalization studies of these and related endogenous proteins in neurons. praja2 is widely distributed in neurons of most regions of the mammalian brain and accumulates within cytoplasmic organelles and at postsynaptic densities (PSDs) of axosomatic synapses *(Nakayama et al., 1995).* Interaction with AKAPs concentrates RIIβ into the soma and dendrites of many types of neurons in the olfactory bulb, basal ganglia, striatum, cerebral cortex, and other forebrain regions *(Tunquist et al., 2008; Zhong et al., 2009).* Accordingly, we analyzed the distribution patterns of praja2, RIIβ and calmodulin-dependent kinase IIα (CaMKIIα) in different rat brain areas. CaMKIIα is a signalling enzyme abundantly expressed in neurons that selectively define PSDs *(Zhou et al., 2009).* praja2 and CaMKIIα share a similar expression profile and intracellular distribution in most of the neurons from different brain regions, including cortex, corpus striatum, hippocampal subregions CA1 and CA3 and dentate gyrus (DG) (**Fig. 11A**). praja2 is abundantly expressed in pyramidal neurons and in the CA3 region of apical dendrites, whereas RIIβ is present in a few pyramidal neurons and mostly in mossy fibers (**Fig. 11B**). Moreover, praja2 and RIIβ signals are partly co-distributed in dentate granule cells.

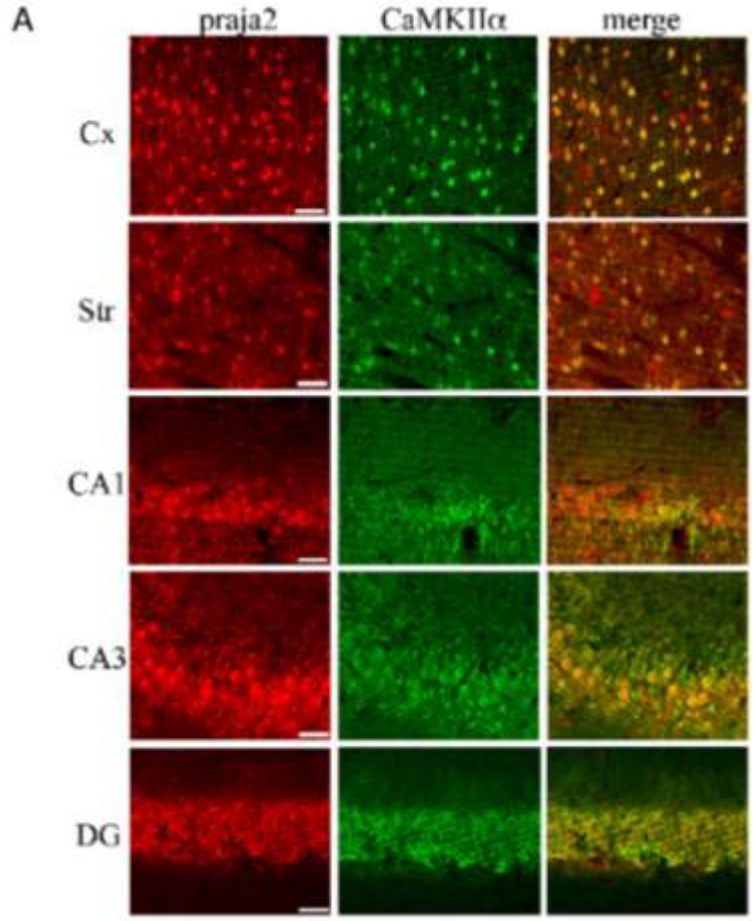
A
praja2
CaMKIIα
merge
Cx
Str
CA1
CA3
DG

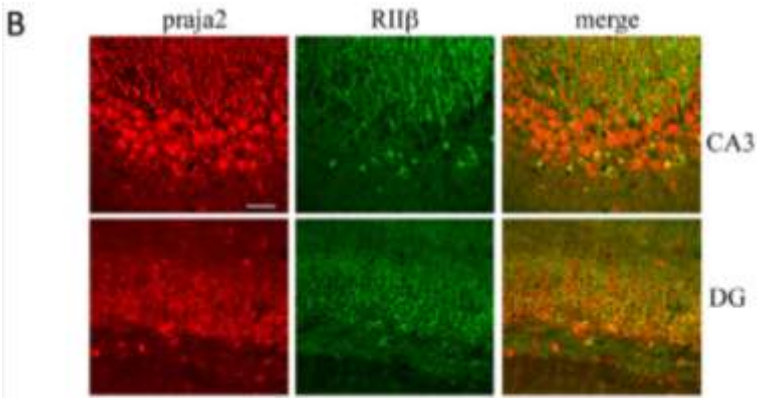
B
praja2
RIIβ
merge
CA3
DG

Figure 11. Distribution of praja2, CaMKIIα and RIIβ in rat brain. (**A**) distribution of praja2 and CaMKII in the brain. Sections from cerebral cortex (Cx), striatum (Str), hippocampus (CA1, CA3) and dentate gyrus (DG) were doubly immunostained with anti-praja2 and anti-CaMKIIα antibodies. Images were collected by confocal microscopy. Scale bar= 50 μm. (**B**) Sections from CA3 and dentate gyrus (DG) were double immunostained with anti-praja2 and anti-RIIβ antibodies. Images were collected by confocal microscopy. Scale bar: 50 μm.

2.6 Endogenous praja2 and RII colocalize in neuronal cells

Colocalization of RII subunits and praja2 was investigated by *in situ* immunostaining of primary hippocampal neurons. Triple immunofluorescence staining using anti-praja2, anti-RIIβ and anti-CaMKIIα antibodies, demonstrates a partial colocalisation of praja2, RIIβ and CaMKIIα signals at postsynaptic sites (**Fig. 12A**). We also investigated colocalization of endogenous RIIβ and praja2 in human neuroblastoma cells (SHSY-5Y). Immunostaining using anti-praja2 and anti-RIIβ antibodies shows colocalization signal of these proteins at Golgi-centrosome and partial colocalization at plasma membrane and some tiny vescicules in cytoplasm (**Fig. 12B**).

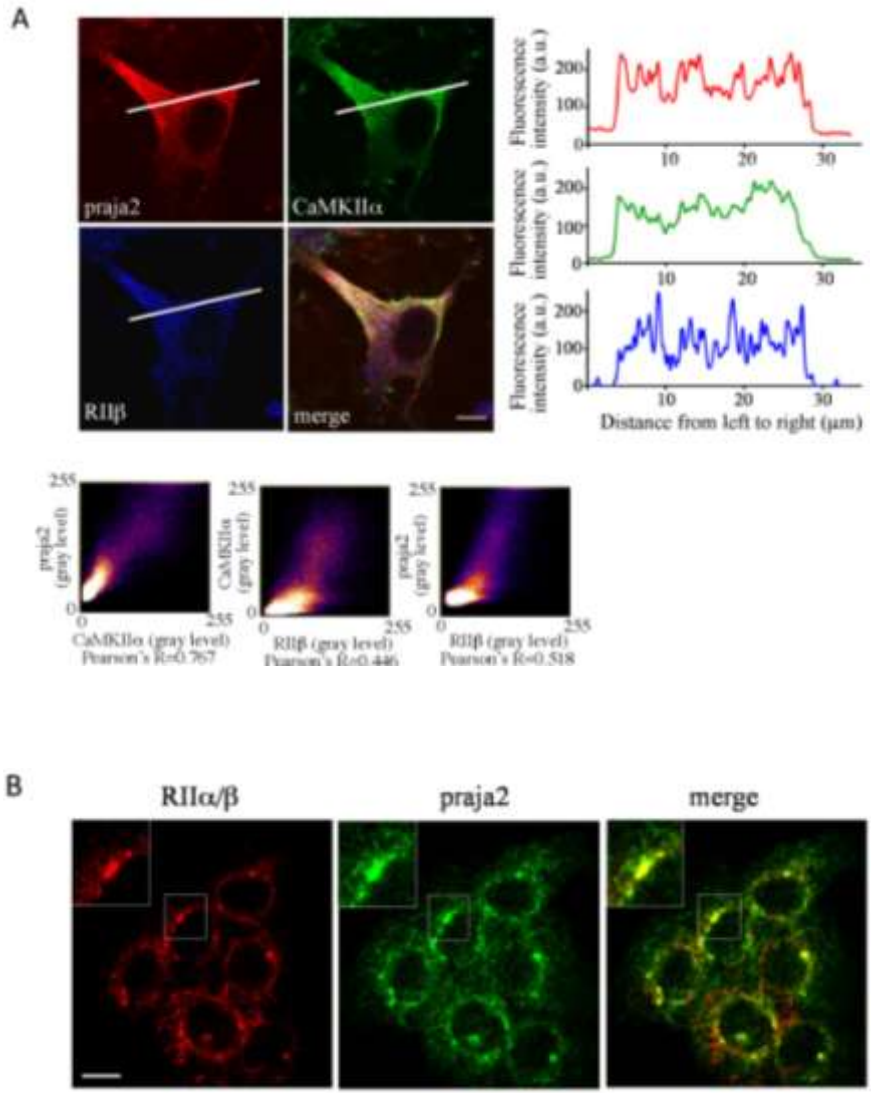

Figure 12. praja2 and RIIβ colocalize in neuronal cells. (**A**) Primary hippocampal neurons were subjected to triple immunofluorescence with rabbit polyclonal anti-praja2, monoclonal mouse anti-CaMKIIα and goat polyclonal anti-RIIβ antibodies. Right panels: profile plots are referred to the cross line shown in the panels and express the intensity (a.u., arbitrary units) of fluorescence from left to right. Lower panels: Pearson's coefficients between praja2, RIIβ and CaMKIIα. Scale bar: 10 μm. (**B**) immunostaining showing coexpression of praja2 and RIIβ in human neuroblastoma cells SHSY-5Y. Colocalization Pearson's coefficient praja2-RII$\beta = 0.51$. Scale bar: 20 μm.

2.7 Expression of exogenous praja2 redistributes endogenous RII subunits

Next we investigated colocalization of RII subunits and exogenous praja2 by *in situ* immunostaining of human neuroblastoma cells (SHSY-5Y). Expression of flag-praja2 redistributed RII subunits from the Golgi-centrosome area to the cytoplasm and cell membrane, compared to control untransfected cells, and partial colocalization of praja2-flag and RII signals could be assigned (**Fig. 13A**). As controls, praja2 mutant lacking the PKA binding domain (Δ531-708-flag) was used (**Fig. 13A**). Similarly, a praja2-GFP fusion promoted relocalization of RII subunits (in HEK293 cells) from intracellular pools to focal points at the plasma membrane, where both signals overlapped (**Fig. 13B, upper panels**). No significant changes of R localization were evident in cells transfected with GFP (**Fig. 13B, lower panels**).

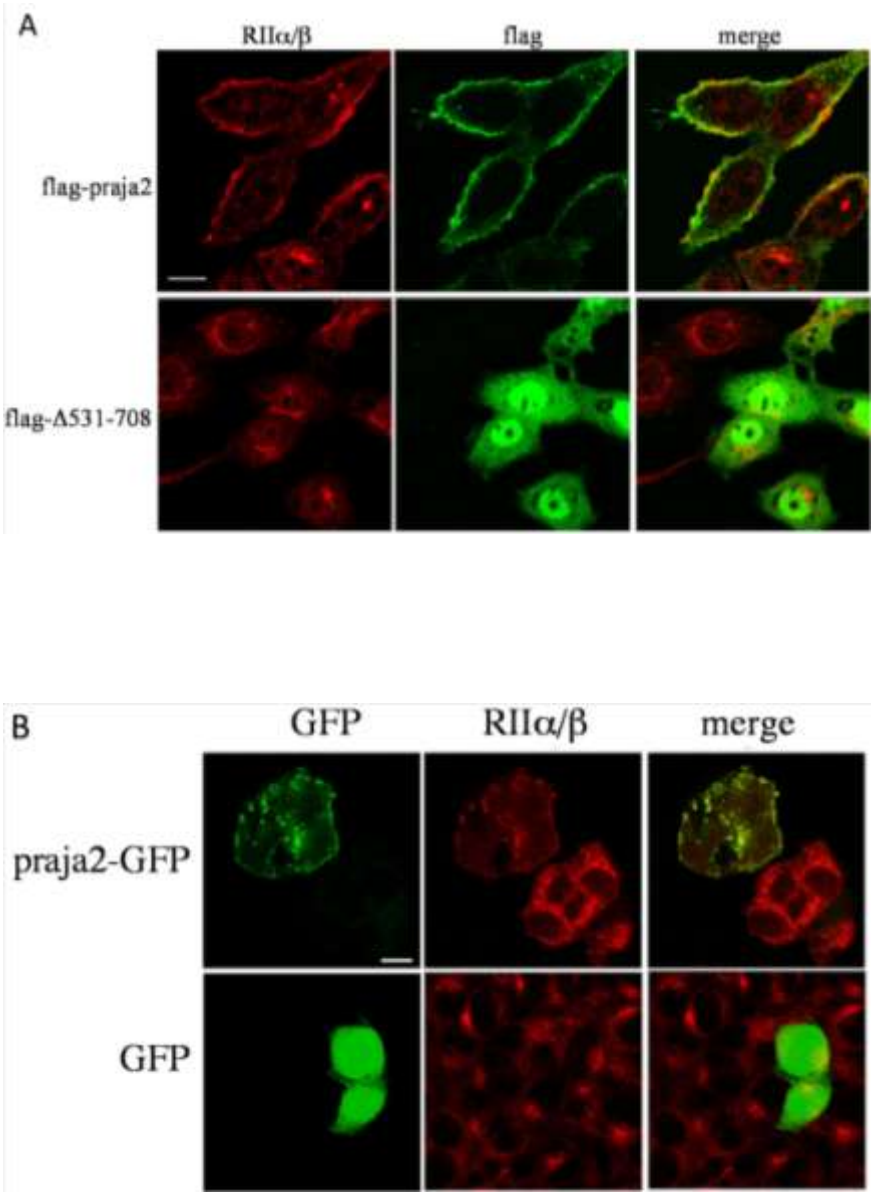

Figure 13. Exogenous praja2 relocalize RII to the plasma membrane. (**A**) Human neuroblastoma cells (SHSY-5Y) were transiently transfected with praja2-flag or its deletion mutant (Δ531-708). 24 hours from transfection, cells were fixed and doubly immunostained with anti-RIIα/β and anti-flag antibodies. 12 hours before harvesting cells were treated with MG132 (10μM). Fluorescent images were collected and analyzed by confocal microscopy. A merged composite is shown. Scale bar: 20 μm. (**B**) HEK293 cells were transiently transfected with praja2-GFP (upper panels) or GFP (lower panels). 24 hours from transfection, cells were fixed and immunostained with anti-RIIα/β. Scale bar: 20 μm.

2.8 praja2 induces proteolysis of R subunits

We hypothesized that praja2, as an E3 ligase, should destabilise R subunits. To confirm this idea, HEK293 cells were transiently co-transfected with expression vectors encoding praja2-flag and with hemaglutinin (HA)-tagged RIIα (**Fig. 14A**), myc-RIIβ (**Fig. 14B**) or HA-RIα (**Fig. 14C**), and results analysed by immunoblot. Indeed, wild type praja2 or a praja2 mutant carrying cysteine 634 substituted to alanine significantly reduced the levels of co-expressed R subunits. In contrast, the concentrations of R subunits in cells expressing praja2rm were similar to those of control cells. praja2-induced degradation of RIα subunits was reversed by MG132 (**Fig. 14D**), indicating that praja2-dependent Rs degradation is mediated by proteasome. Similarly, endogenous RIIα/β and RI subunits were degraded by overexpressed praja2-flag, but not by the praja2-flag RING mutant (**Fig. 14E**).

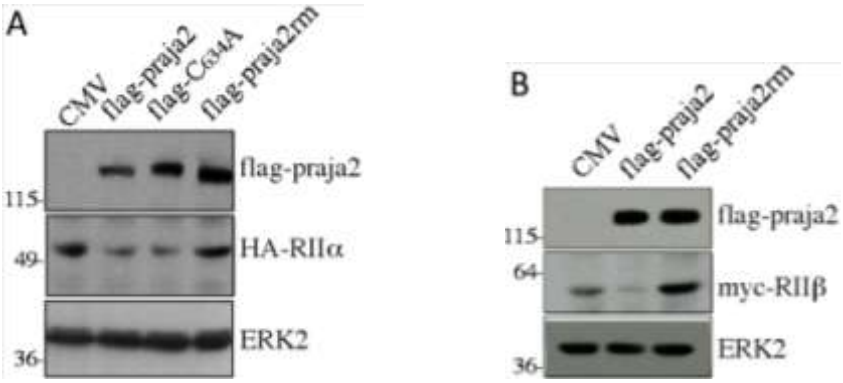

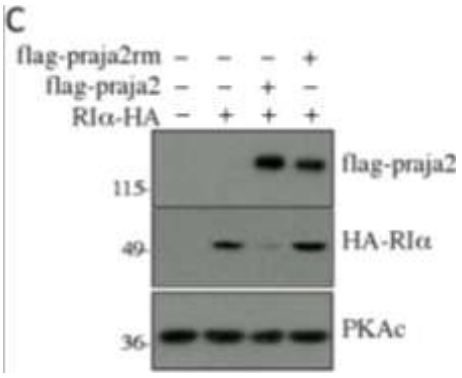
C
flag-praja2rm – – – +
flag-praja2 – – + –
RIα-HA – + + +
115
49
36
flag-praja2
HA-RIα
PKAc

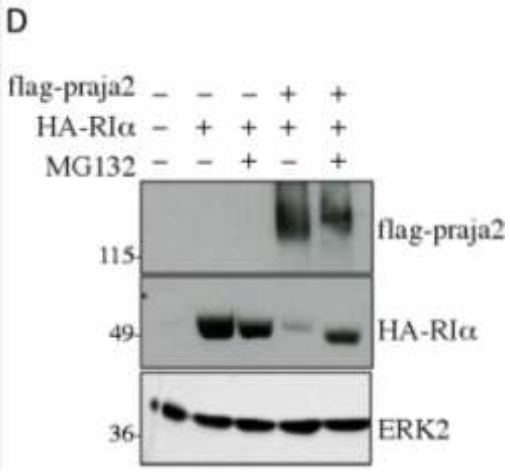
D
flag-praja2 – – – + +
HA-RIα – + + + +
MG132 – – + – +
115
49
36
flag-praja2
HA-RIα
ERK2

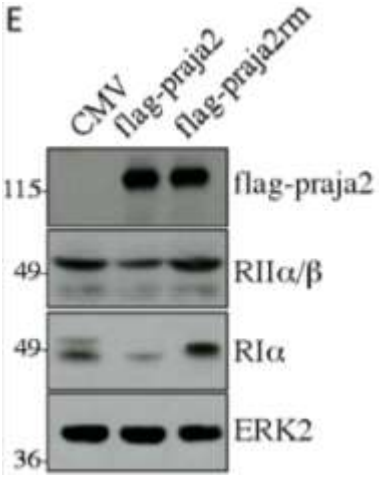
E
CMV
flag-praja2
flag-praja2rm
115
49
49
36
flag-praja2
RIIα/β
RIα
ERK2

Figure 14. praja2 triggers degradation of R subunits. (**A-C**) HEK293 cells were transiently co-transfected with HA-RIIα (**A**), myc-RIIβ (**B**) or HA-RIα (**C**) and praja2-flag expression vectors. In (A), two RING mutants were used: praja-Cys634A and praja2rm. 24 hours following transfection, cells were harvested and lysed. Lysates were immunoblotted with the indicated antibodies. (**D**) Same as (C), except the cells were treated for 8 hours with MG132 (20μM) before harvesting. (**E**) Immunoblot analysis of endogenous R subunits on lysates from cells transiently transfected with praja2-flag vectors. ERK2 was used as loading control.

2.9 praja2 ubiquitinates RII subunits

E3 ubiquitin ligase praja2 triggers R subunits degradation, so we next asked if praja2 ubiquitinates R subunits. HEK293 cells were co-transfected with praja2-flag, praja2rm-flag, myc-RIIβ and HA-ubiquitin vectors. Cells were treated with MG132 and lysates were immunoprecipitated with anti–myc antibody and immunoblotted with anti-HA, anti-RIIα/β and anti-flag antibodies. Expression of praja2, but not of praja2rm, induced accumulation of poly-ubiquitinated myc-RIIβ (**Fig. 15A**). Since degradation of RII by praja2 is enhanced by cAMP (see below), we determined if praja2 was required for RII ubiquitination in forskolin-stimulated cells. In control cells, immunoprecipitated RIIα/β ubiquitination was potentiated by forskolin (synthetic adenylyl cyclase activator) and IBMX (3-isobutyl-1-methylxanthine, phosphodiesterase inhibitor) treatment (**Fig. 15B**). Depletion of endogenous praja2 using specific siRNA, drastically reduced RIIα/β ubiquitination, both in untreated and forskolin stimulated cells. An *in vitro* ubiquitination assay confirmed that RIIα is, indeed, a direct substrate of praja2 (**Fig. 15C**). In contrast, praja2rm and a praja2 mutant lacking the PKA phosphorylation sites (S342A, T389A, see below) failed to ubiquitinate RII *in vitro*.

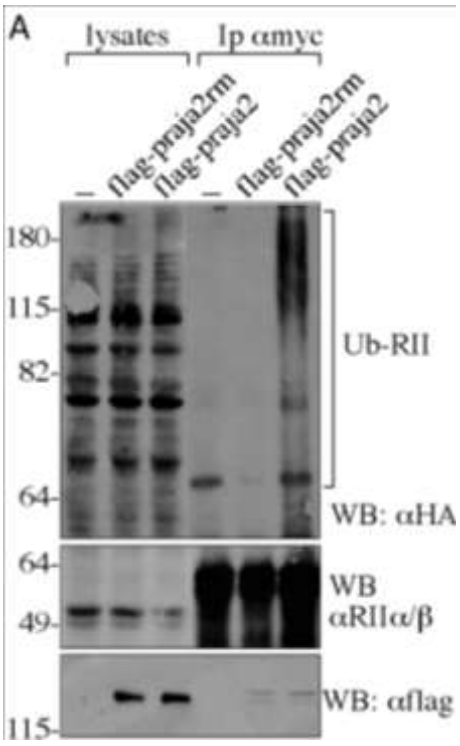
A
lysates
Ip αmyc
–
flag-praja2rm
flag-praja2
–
flag-praja2rm
flag-praja2
180
115
82
64
Ub-RII
WB: αHA
64
49
WB
αRIIα/β
115
WB: αflag

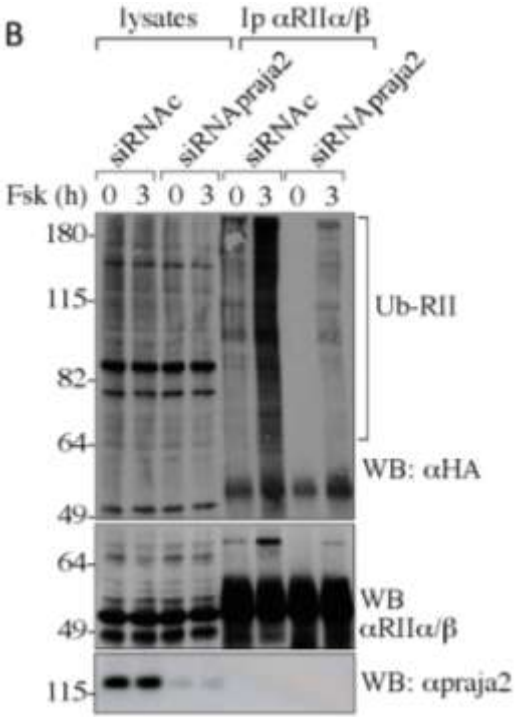
B
lysates
Ip αRIIα/β
siRNAc
siRNApraja2
siRNAc
siRNApraja2
Fsk (h) 0 3 0 3 0 3 0 3
180
115
82
64
49
Ub-RII
WB: αHA
64
49
WB
αRIIα/β
115
WB: αpraja2

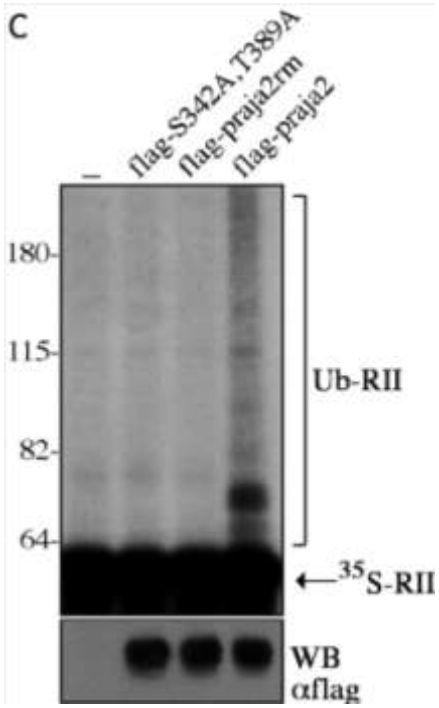

Figure 15. praja2 ubiquitinates RIIα/β subunits. (**A**) HEK293 cells were transfected with HA-ubiquitin, RIIβ-myc and praja2 or praja2rm. 24 hours after transfection, cells were treated with MG132 (20 μM) for 8 hours. Lysates were immunoprecipitated with anti−myc and immunoblotted with anti-HA, anti-RIIα/β and anti-flag antibodies. (**B**) HEK293 cells were transfected with HA-tagged ubiquitin. Where indicated, control (siRNAc) or SMARTpool siRNApraja2 (siRNApraja2) was included in the transfection mix. 24 hours after transfection, cells were either left untreated or stimulated with forskolin (40 μM) and IBMX (0.5 mM) for 3 hours, in the presence of MG132 (20 μM). Lysates were immunoprecipitated with anti-RIIα/β and immunoblotted with anti-HA, anti-RIIα/β and anti-praja2 antibodies. Arrow indicates endogenous praja2. (**C**) *In vitro* translated, ^{35}S-labeled RIIα was incubated with his6-tagged ubiquitin, in the presence or absence of E1, UbcH5c (E2) and anti-flag precipitates from HEK293 extract transiently transfected with praja2-flag, praja2rm-flag or S342A, T389A-flag. The reaction mix was denatured, size-fractionated on 7% SDS-PAGE, and analyzed by autoradiography. A fraction of the reaction mixture was immunoblotted with anti-flag antibody (lower panel).

2.10 Regulated binding of PKA to praja2 by cAMP signaling

Ubiquitination and consequent proteolysis of R subunits by praja2 are stimulated by cAMP, suggesting that dissociation of PKA holoenzyme is a prerequisite for R degradation. Regulation of praja2 activity by PKAc might also contribute to proteolytic turnover of R subunits. To address this issue, we performed immunostaining analysis of PKAc in neurobloastoma cells SHSY-5Y overexpressing praja2. praja2 redistributed PKAc from the Golgi-centrosome area to the cytoplasm and plasma membrane (**Fig. 16A**). We also performed coimmunoprecipitation assays to confirm that PKAc interacts with praja2. A praja2•PKAc complex could be isolated from serum-deprived cells (**Fig. 16B**). Forskolin treatment increased the amount of PKAc recovered in the anti-praja2 precipitates. This effect was reversed by pre-treating the cells with H89, a potent PKA inhibitor. In addition, forskolin triggered complex formation of praja2•PKAc resulted in phosphorylation of praja2 by the associated kinase (**Fig. 16B, lower panels**). We then performed an independent test to verify the cAMP-dependent interaction of PKA with praja2. Thus, cAMP-coupled agarose beads co-precipitated endogenous PKA

holoenzyme in complex with overexpressed praja2-flag (**Fig. 16C** and **Fig. 16D**).

The resin-coupled cAMP analogue competes with endogenous cAMP in binding to R subunits, preventing dissociation of PKA holoenzyme by forskolin or isoproterenol treatment. As a negative control we added excess cAMP (5mM) to mask the cAMP binding sites in the R subunits for precipitation (**Fig. 16E**). Under basal conditions, overexpressed praja2-flag (**Fig. 16E** and **Fig. 16F**) were coprecipitated with endogenous R-PKAc complexes. However, pre-treating the cells with forskolin or isoproterenol for 15 minutes increased the amount of recovered PKA•praja2-flag complexes (**Fig. 16E** and **Fig. 16F**). These results confirm the idea that praja2 forms stable complexes with the PKA holoenzyme and that cAMP elevation further enhances the formation of the PKA•praja2 complex.

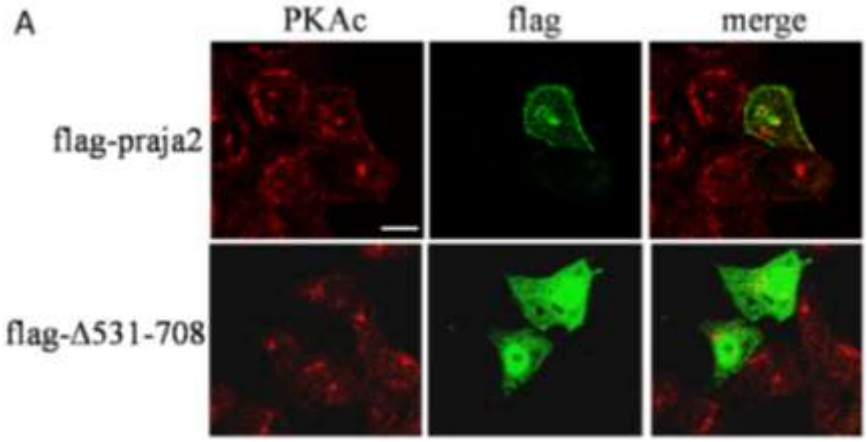

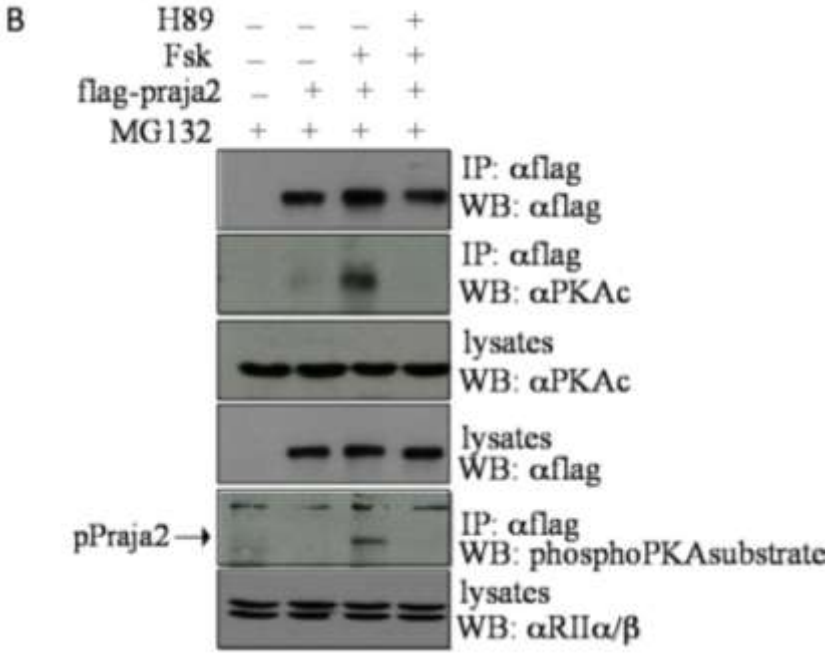
B
H89 – – – +
Fsk – – + +
flag-praja2 – + + +
MG132 + + + +
IP: αflag
WB: αflag
IP: αflag
WB: αPKAc
lysates
WB: αPKAc
lysates
WB: αflag
pPraja2
IP: αflag
WB: phosphoPKAsubstrate
lysates
WB: αRIIα/β

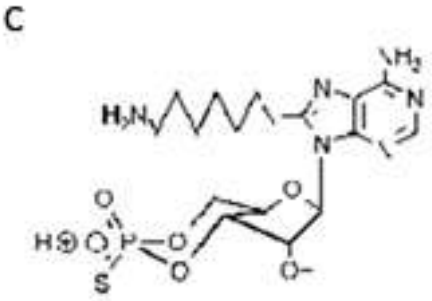
C

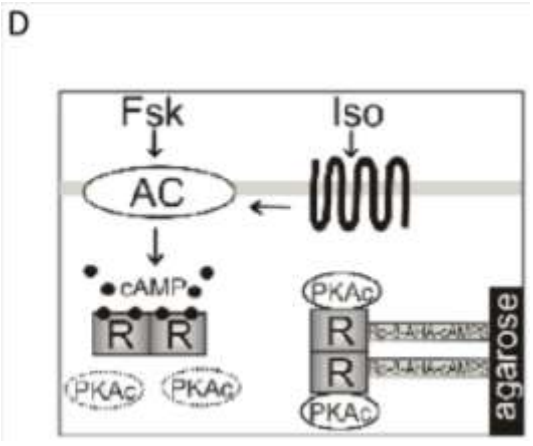
D
Fsk
Iso
AC
cAMP
R
R
PKAc
PKAc
PKAc
R
R
PKAc
agarose

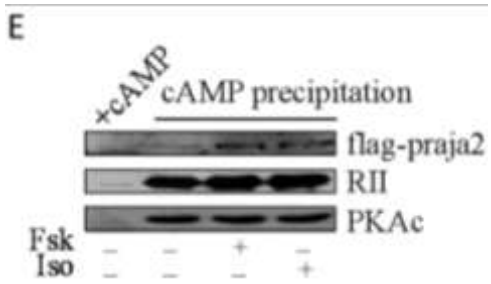

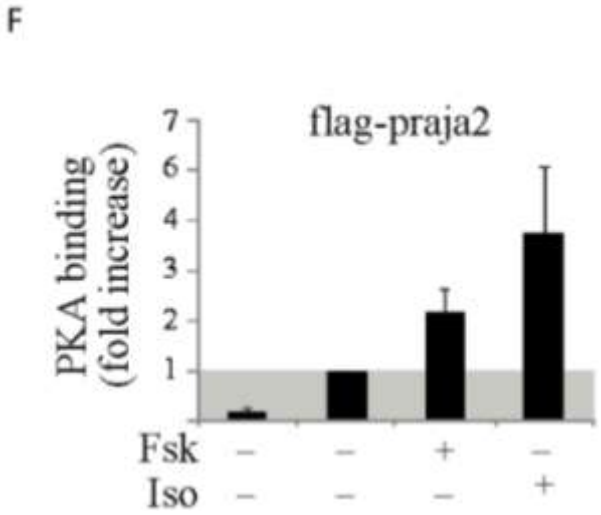

Figure 16. PKA-praja2 regulated interaction. (**A**) SHSY-5Y cells were transiently transfected with praja2-flag or Δ531-708-flag vector and immunostained with anti-flag and anti-PKAc antibodies. (**B**) Lysates from HEK293 cells expressing praja2-flag and treated with MG132 for 12 hr were immunoprecipitated with anti-flag antibody. The precipitates were immunoblotted with the indicated antibodies. Where indicated, cells were treated with forskolin (Fsk 40 μM) and IBMX (0.5 mM) for 30 min before harvesting, in absence or presence of H89 (10 μM). (**C**) Schematic structure of the cAMP analog, Rp-8-AHA-cAMP. (**D**) Schematic illustration of the cAMP precipitation strategy: Resin coupled cAMP analogue binds endogenous R subunits and promotes PKA holoenzyme re-association following forskolin (Fsk) or isoproterenol (Iso) treatment (R•PKAc; AC, adenylyl cyclase). (**E**) cAMP precipitation of endogenous PKA subunits using cAMP agarose resin (Rp-8-AHA-cAMP) from β2AR

HEK293 cells transiently expressing praja2-flag in response either to 15 min of forskolin (100 μM) or isoproterenol (10 μM) treatment. In the negative control experiment we added excess of cAMP (5 mM) to the lysates to mask the cAMP binding sites in the R subunits. Immunoblot analysis was done with anti-RII, anti-PKAc and anti-flag antibodies. (**F**) Densitometric quantification of the fold enrichment of complex formation of R subunits and praja2 in response to forskolin and isoproterenol. Results are presented as means ± S.E.M. from three independent experiments.

2.11 PKAc phosphorylates praja2 at Ser342 and Thr389

We assessed if praja2 is a substrate of PKAc. Primary sequence analysis predicts the presence of two PKA phosphorylation sites within the core region of praja2 (Ser 342 and Thr 389) (**Fig. 17A, upper panel**). HEK293 cells transiently transfected with praja2-flag or praja2 S342A,T389A mutant were treated with forskolin and lysates were immunoprecipitate with anti-flag antibody and immunoblotted with phosphoSer/Thr PKA substrates and flag antibodies. Substitution of both residues with alanine (S342A, T389A) inhibited forskolin-induced praja2 phosphorylation (**Fig. 17A, lower panels**). In vitro kinase assays demonstrated that purified PKAc directly phosphorylates immunoprecipitated wild type praja2, but not the S342A, T389A mutant, confirming these residues as the major PKA phosphorylation sites (**Fig. 17B**).

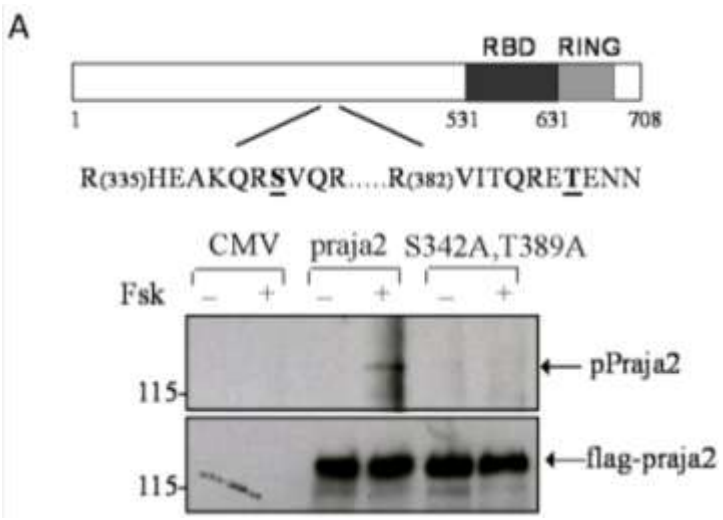

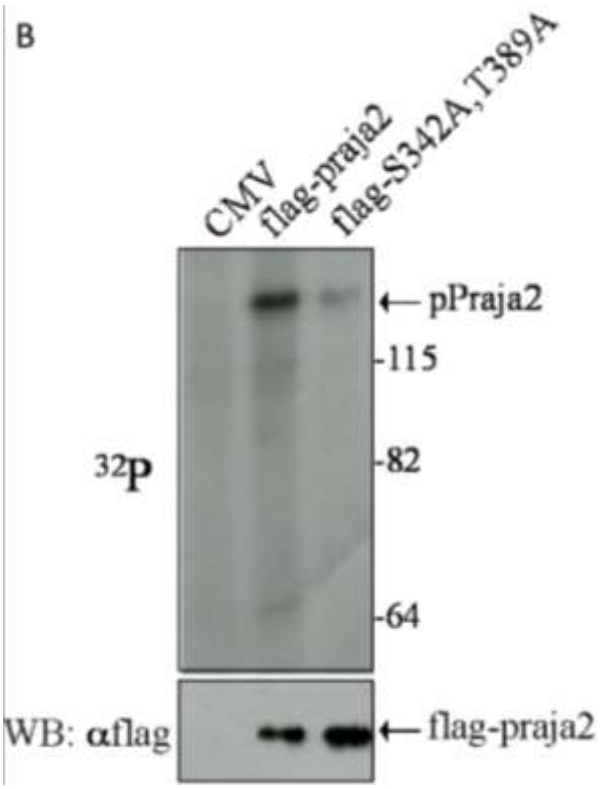

Figure 17. PKAc phosphorylates praja2 at Ser342 and Thr389. (**A**) Schematic diagram of praja2, including protein sequence surrounding the putative PKA consensus sites. Serine 342 and Threonine 389 are underlined. HEK293 cells transiently transfected with empty vector (CMV), praja2-flag or praja2 S342A,T389A mutant were serum deprived overnight and treated with forskolin (40 μM) and IBMX (0.5 mM) for 30 min before harvesting. Lysates were immunoprecipitates with anti-flag antibody and immunoblotted for the detection of phosphoSer/Thr PKA substrates and flag antibodies. (**B**) praja2-flag and its mutant praja2 S342A,T389A were immunoprecipitated from cell lysates. The precipitates were incubated in kinase buffer for 10 min with purified PKAc and ATP/[^{32}P]-γATP and resolved on SDS-PAGE. [^{32}P]-labeled praja2 was visualized by autoradiography. An aliquot of the samples was immunoblotted with anti-flag antibody.

2.12 Phosphorylation of praja2 is required for R degradation

cAMP signaling stimulation induces Rs degradation by praja2 ubiquitination and our data reveal that PKAc directly phosphorylates praja2. This events suggest a crucial role of PKAc mediated phosphorylation of praja2 in activating praja2 E3 ligase activity. To address this event we performed co-immunoprecipitation assays using HEK293 cells transiently transfected with praja2-flag or praja2 S342A,T389A mutant and treated with forskolin or left untreated. Lysates were immunoprecipitate with anti-RIIα/β antibody. These experiments confirmed that praja2 phosphorylation is required for its cAMP-mediated interaction with R subunits (**Fig. 18A**). Moreover, expression of S342A, T389A mutant stabilizes RII subunits, even in cells stimulated with forskolin and IBMX (**Fig. 18B**). This implies that PKA activity regulates the abundance of compartmentalized pools of R subunits via praja2 phosphorylation and recruitment to R subunits, leading to subsequent R proteolysis.

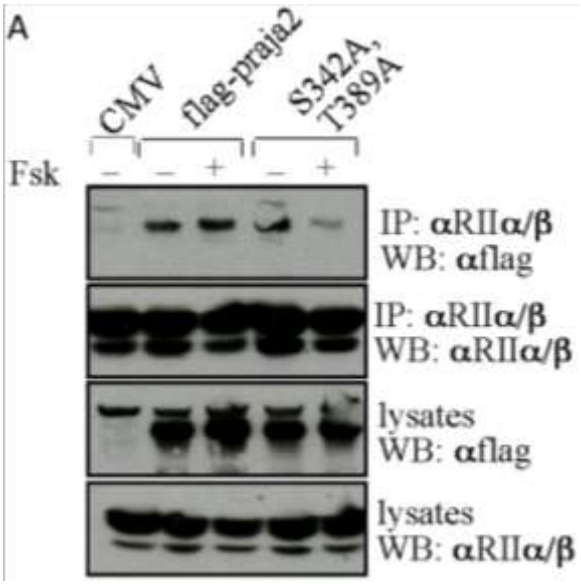
A
CMV
flag-praja2
S342A, T389A
Fsk
– – + – +
IP: αRIIα/β
WB: αflag
IP: αRIIα/β
WB: αRIIα/β
lysates
WB: αflag
lysates
WB: αRIIα/β

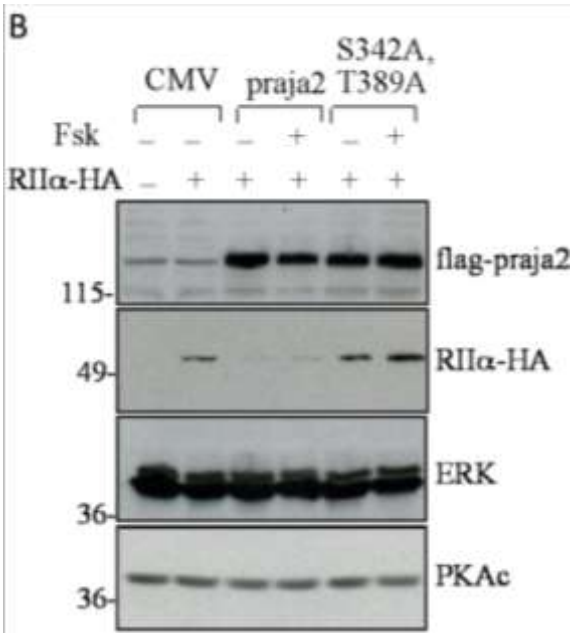
B
CMV
praja2
S342A, T389A
Fsk
– – – + – +
RIIα-HA – + + + + +
115-
49-
36-
36-
flag-praja2
RIIα-HA
ERK
PKAc

Figure 18. PKAc mediated phosphorylation of praja2 activate E3 ligase activity. (**A**) HEK293 cells transiently transfected with the indicated vectors were serum-deprived overnight and stimulated with forskolin (40μM) for 30 min. Lysates were immunoprecipitated with anti-RIIα/β antibodies. Precipitates and lysates were immunoblotted anti-RIIα/β and anti-flag antibodies. (**B**) Lysates from serum-deprived and forskolin-treated (40μM) cells transiently co-transfected with HA-RIIα and empty vector (CMV), praja2-flag or praja2 S342A,T389A mutant were immunoblotted with anti-HA and anti-flag antibodies. ERK2 was used as loading control.

2.13 praja2 regulates PKA-induced CREB phosphorylation in cells

The coupling of adenylate cyclase activation at the cell membrane to mRNA induction involves dissociation of PKA holoenzyme, translocation of PKAc to the nucleus, phosphorylation of the transcription factor CREB at Ser133 and phosphoCREB/coactivator-dependent activation of nuclear gene transcription *(Lonze et al., 2002; Feliciello et al., 1997).* The data shown above indicate that praja2 mediates cAMP-dependent degradation of R subunits, prolonging the time of PKAc activation. Thus, we would predict that depletion of praja2 decreases PKAc signalling to nuclear targets (i.e. CREB). Endogenous praja2 was depleted by transfecting siRNApraja2, as confirmed by immunofluorescence (**Fig. 19A**) and immunoblot analyses (**Fig. 19B**). In control cells, most RII staining was concentrated at the Golgi-centrosome area and the perinuclear region. praja2 down-regulation dispersed RIIβ throughout the cytoplasm (**Fig. 19A**). The physiological significance of praja2 down-regulation on nuclear cAMP signalling was evaluated by analysis of CREB phosphorylation at Ser133 *in situ*. In control cells, forskolin stimulation increased the number of phosphoSer133-CREB positive nuclei in a time-dependent manner (**Fig. 19B** and **Fig.**

19C). In contrast, a nearly two-fold decline in phosphoSer133-CREB positive nuclei was seen in cells transfected with siRNApraja2 at both time points of forskolin stimulation. Down-regulation of praja2 by siRNApraja2 prevented the forskolin-induced decline of RII subunits and inhibited CREB phosphorylation (**Fig. 19D** and **Fig. 19E**). Coexpression of praja2-flag, but not of its mutant Δ531-708, reversed the effects of siRNApraja2 (**Fig. 19F**).

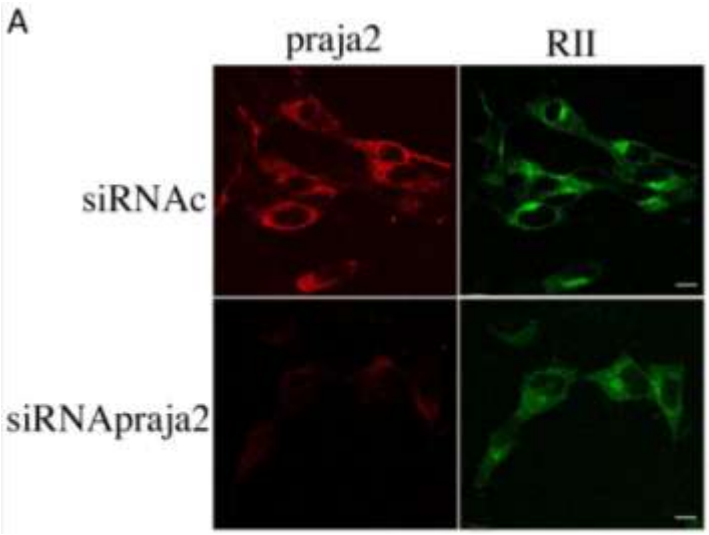

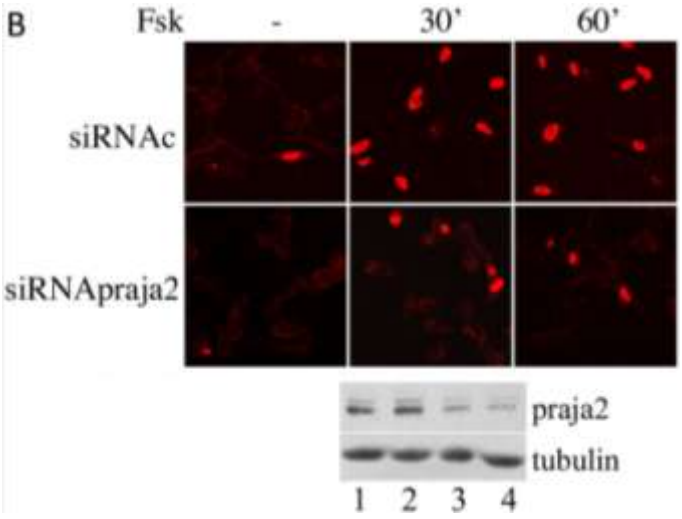
B
Fsk
-
30'
60'
siRNAc
siRNApraja2
praja2
tubulin
1 2 3 4

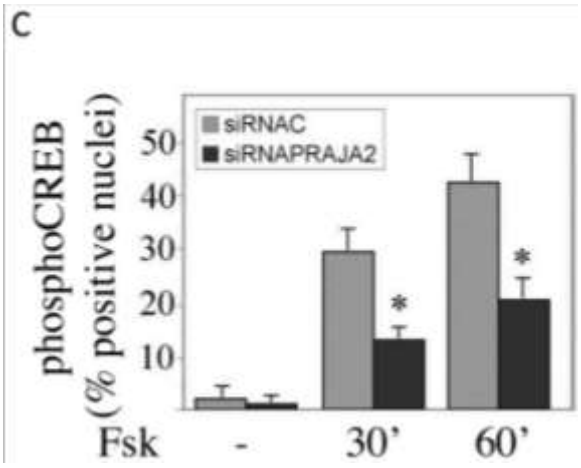
C
phosphoCREB
(% positive nuclei)
siRNAC
siRNAPRAJA2
50
40
30
20
10
*
*
Fsk
-
30'
60'

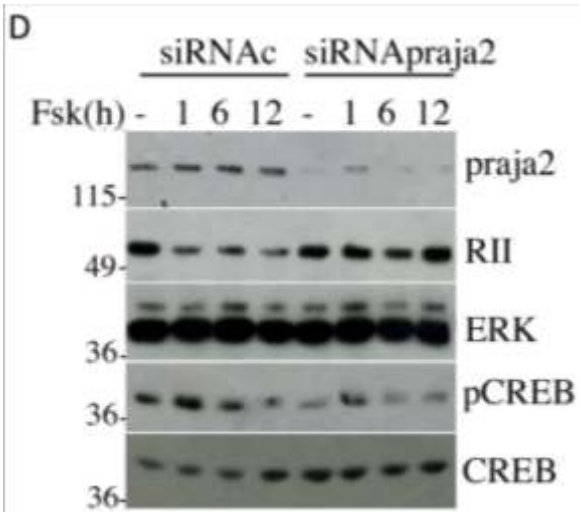
D
siRNAc
siRNApraja2
Fsk(h) - 1 6 12 - 1 6 12
115-
49-
36-
36-
36-
praja2
RII
ERK
pCREB
CREB

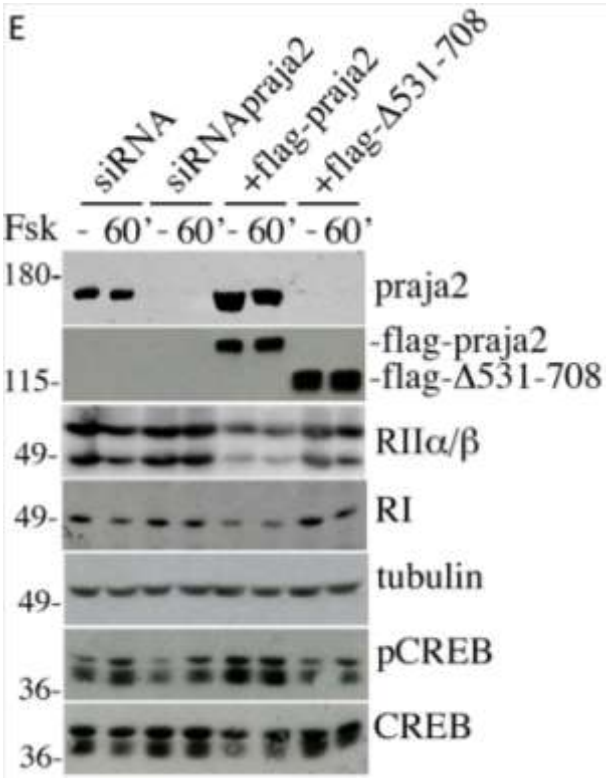

Figure 19. praja2 controls PKA signalling. (**A**) Double immunofluorescence for praja2 and RIIβ in human neuroblastoma cells SHSY-5Y transiently transfected with siRNAc or siRNApraja2. Scale bar: 20 μm. Scale bar: 20 μm. (**B**) 24 hours from transfection, cells were serum deprived overnight and stimulated with forskolin (40 μM) and IBMX (0.5 mM) for 30 min and 60 min. Formalin-fixed cells were immunostained with anti-phosphoSer133 antibody. Immunoblots (lower panels) show the expression of praja2 in siRNAc (lanes 1, 2) and siRNA-transfected (lanes 3, 4) cells, left untreated (lanes 1, 3) or stimulated with forskolin for 60 min (lanes 2, 4). (**C**) Quantitative analysis of the experiments shown in B. The data are expressed as mean ± S.E.M. of three independent experiments made in triplicate. 200-250 cells were scored in each set of experiments. *P <0.01 versus control (siRNAc). (**D**) Lysates from control (siRNAc) or siRNApraja2-transfected cells were serum deprived overnight. Before harvesting, cells were left untreated or stimulated with forskolin (Fsk) (40μM) and IBMX (0.5mM) for the indicated times. Lysates were immunoblotted with the indicated antibodies. (**E**) Immunoblot analysis of lysates from control (siRNAc) or siRNApraja2-transfected cells. Before harvesting, cells were serum

deprived overnight and left untreated or stimulated with forskolin (Fsk) (40μM) and IBMX (0.5mM) for 30 min. Where indicated, praja2-flag vectors (wild type and its mutant Δ531-708) were included in the transfection mixture. Lysates were immunoblotted with the indicated antibodies.

2.14 praja2 regulates PKA-induced *c*-fos transcription in cells

Transcription of c-*fos* is mediated by binding of CREB to an upstream cAMPresponsive element (CRE). CREB phosphorylation at Ser133 drives c-fos transcription *(Montminy, 1997).* We monitored the effects of praja2 down-regulation on c-*fos* mRNA synthesis. In control (siRNAc) cells, low levels of c-*fos* mRNA were detected under basal conditions. Activation of adenylate cyclase by isoproterenol (β-agonist hormone) induced a robust and persistent increase of c-*fos* mRNA at 30 min and 60 min following treatment (**Fig. 20A**). Induction of c-*fos* mRNA was reduced several-fold in siRNApraja2-transfected cells. Similar effects on *c-fos* transcription by siRNApraja2 were observed in cells that were stimulated with forskolin (**Fig. 20B**). Rescue experiments confirmed the role of praja2 phosphorylation and activity in the control of cAMP-induced gene transcription. Thus, co-expression of wild type praja2, but not of its mutants (praja2rm and S342A, T389A), rescued c-fos mRNA accumulation in siRNApraja2-transfected cells, at both 60 min and 120 min of stimulation with forskolin (**Fig. 20B**). Moreover, co-expression of PKAc bypassed the block imposed by siRNApraja2 and partially restored *c-fos* levels. These findings strongly suggest that down-regulation of R

subunit by praja2 prolongs the wave of PKAc activation and positively impacts on downstream signalling.

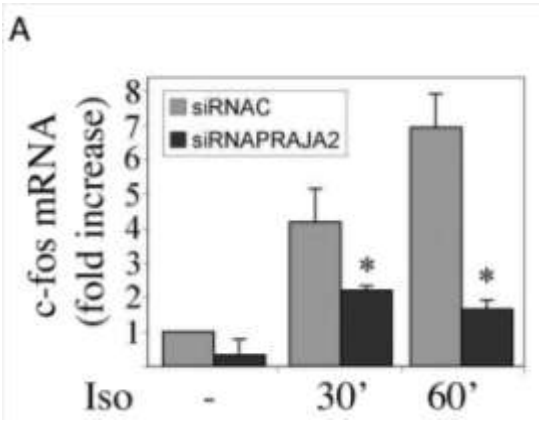

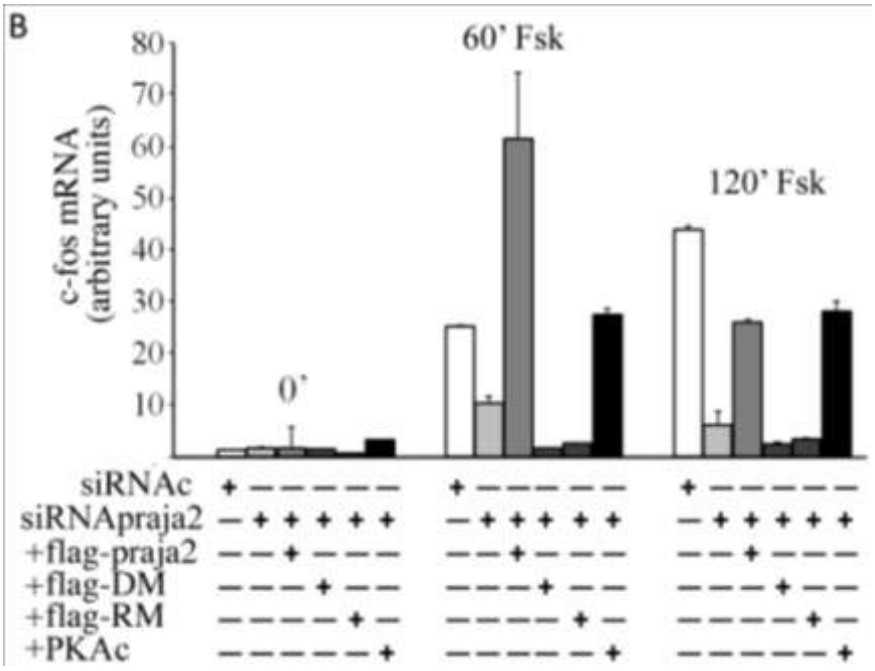

Figure 20. praja2 controls PKA-dependent transcription. (**A-B**) Quantitative RT-PCR showing *c-fos* accumulation in HEK293 cells transfected with siRNAc or siRNApraja2 and stimulated with isoproterenol (1μM) (**A**) or forskolin (40μM) and IBMX (0.1 mM) (**B**) for the indicated time points. Data represent a mean value ± S.E.M. from two independent experiments made in triplicate. Where indicated, vectors for praja2, praja2 S342A,T389A, praja2rm and PKAc were included in the transfection mixture. *P <0.01 versus control (siRNAc).

2.15 praja2 silencing impairs nuclear cAMP signaling in rat brain

praja2 is abundantly expressed in mammalian *brain (Nakayama et al., 1995)* (see above). This prompted us to investigate if down-regulation of praja2 in intact brains would affect nuclear PKAc signalling. siRNApraja2 or siRNAc were perfused intracerebro-ventricularly (icv) in rats (**Fig. 21A**). Intracerebral infusions of siRNApraja2 reduced praja2 levels in areas surrounding the perfused hemispheres (striatum and hippocampus) (**Fig. 21B**). Functional consequences of praja2 down-regulation on cAMP-PKA signalling were evaluated by CREB phosphorylation and *c-fos* transcription in striato-hippocampal areas. Significant amounts of basal phosphoSer133-CREB were evident in control rat brain (**Fig. 21B** and **Fig. 21C**). CREB phosphorylation modestly increased at 30 min after icv infusion of isoproterenol and declined in the next 30 min. *In vivo* silencing of praja2 reduced CREB phosphorylation by about two-fold, both under basal conditions and with isoproterenol treatment. *In situ* immunohistochemistry confirmed the inhibition of CREB phosphorylation in the hippocampal area of siRNApraja2-perfused rat brain, compared to controls (**Fig. 21D** and **Fig. 21E**). Inhibition of CREB phosphorylation by siRNApraja2

provoked a significant down-regulation of isoproterenol-induced *c-fos* transcription (**Fig. 21F**).

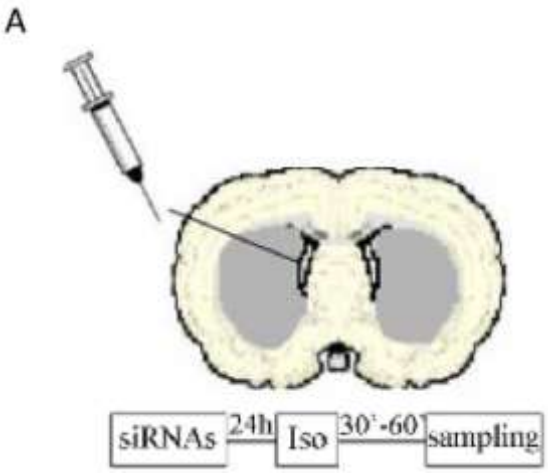

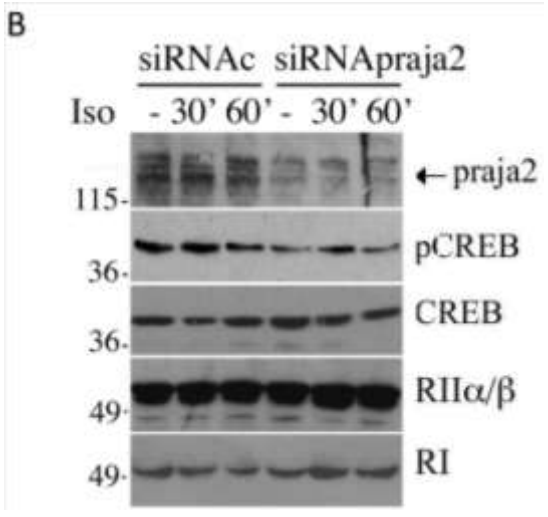

C

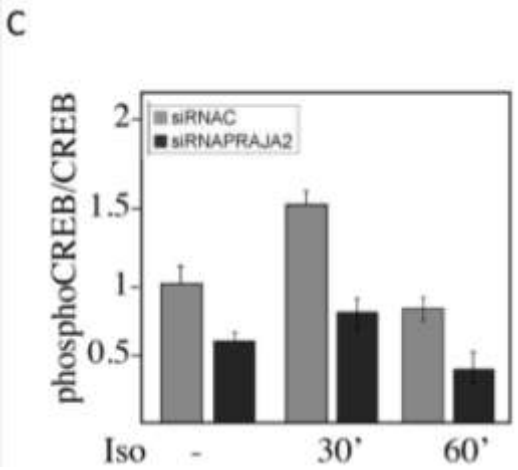
siRNAC
siRNAPRAJA2
phosphoCREB/CREB
2
1.5
1
0.5
Iso
-
30'
60'

D

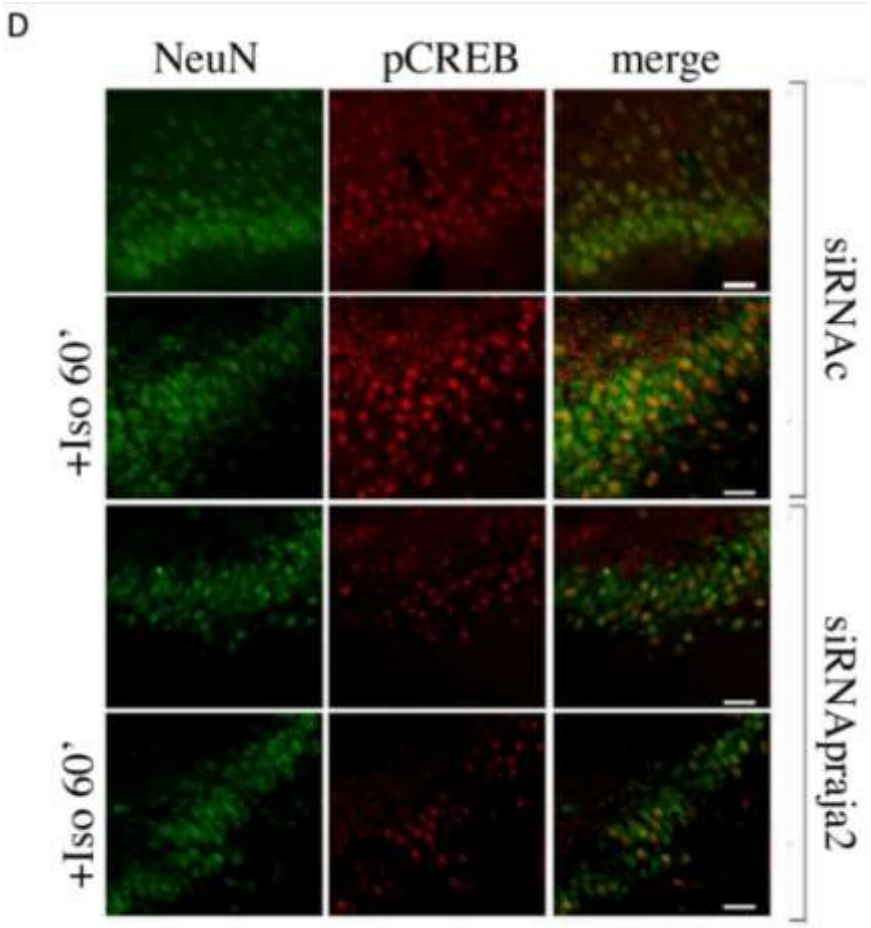
NeuN
pCREB
merge
+Iso 60'
+Iso 60'
siRNAc
siRNApraja2

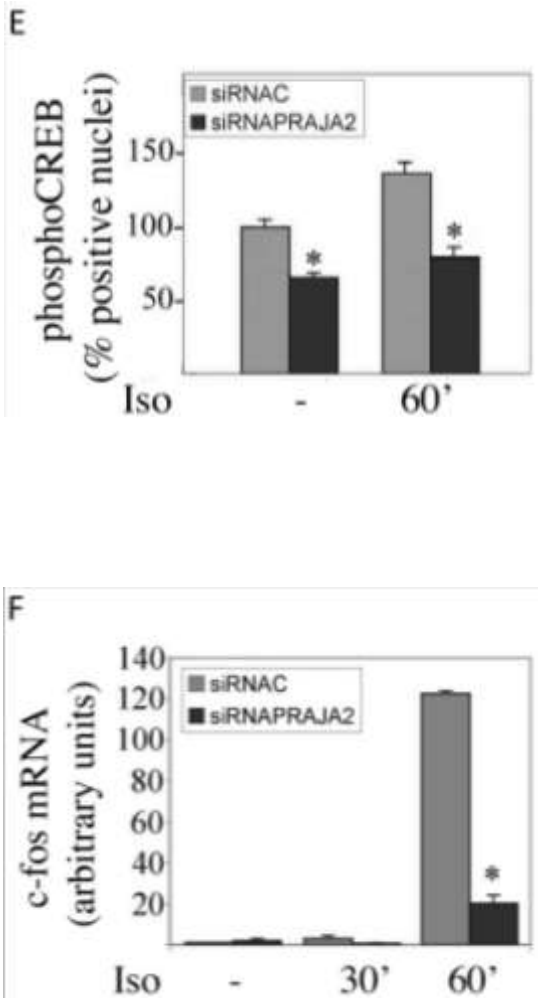

Figure 21. praja2 controls nuclear cAMP signaling in rat brain. (A) Schematic diagram showing intraventricular siRNAs administration in rat brain. Three sequential siRNAs infusions were employed (time points: 0 h, 10 h, 22 h). 24 hours later, isoproterenol was icv infused. Rats were sacrified following 30 min and 60 min isoproterenol exposure. (**B**) Immunoblot analysis of lysates from hippocampal/striatal regions of rat brain intraventricularly perfused with siRNAs and subsequently treated with isoproterenol for the indicated time points. Lysates were immunoblotted with the indicated antibodies. (**C**) Quantitative analysis of phosphoCREB from the experiments shown in (B). The data are expressed as mean ± S.E.M. of three experiments. (**D**) Sections from hippocampal regions of rat brain perfused with siRNAs and treated with isoproterenol as in (C) were doubly immunostained with anti-phosphoCREB and anti-NeuN antibodies. The images were collected and

analysed by confocal microscopy. Scale bar: 50 μm. (**E**) Quantitative analysis of the experiments shown in (D). The data are expressed as mean ± S.E.M. of two independent experiments. 300-350 cells were scored in each set of experiments. *P <0.05 versus control (siRNAc). (**F**) Quantitative RT-PCR showing *c-fos* accumulation in the striatum. Data represent a mean value ± S.E.M. from two independent experiments made in duplicate that gave similar results. *P <0.01 versus control (siRNAc).

2.16 praja2 silencing impairs L-LTP in rat brain

Finally, we investigated the electrophysiological consequences of praja2 down-regulation by monitoring LTP at perforant pathway to granule cell synapses (PP-DG). Firstly, we studied the early, PKA-independent, phase of LTP (E-LTP) induced by one train of HFS *(Malleret et al., 2010)*. We found similar E-LTP in both siRNAc and siRNApraja2-treated rats (50–60 min post-HFS: siRNAc, 155 ± 21%; siRNApraja2, 161 ± 9%, $p > 0.05$) (**Fig. 22A**). Next, we studied the late phase of LTP (L-LTP), that typically requires the activation of cAMP-PKA *(Malleret et al., 2010)*, by using a theta burst stimulation (TBS) pattern. Interestingly, this protocol reliably induced sustained L-LTP in controls but not in siRNApraja2-treated rats (150–160 min post-TBS: siRNAc, 177 ± 11%; siRNApraja2, 123 ± 11%, $p < 0.05$) (**Fig. 22B**). These results suggest that praja2 activity is essential for long-term memory processes.

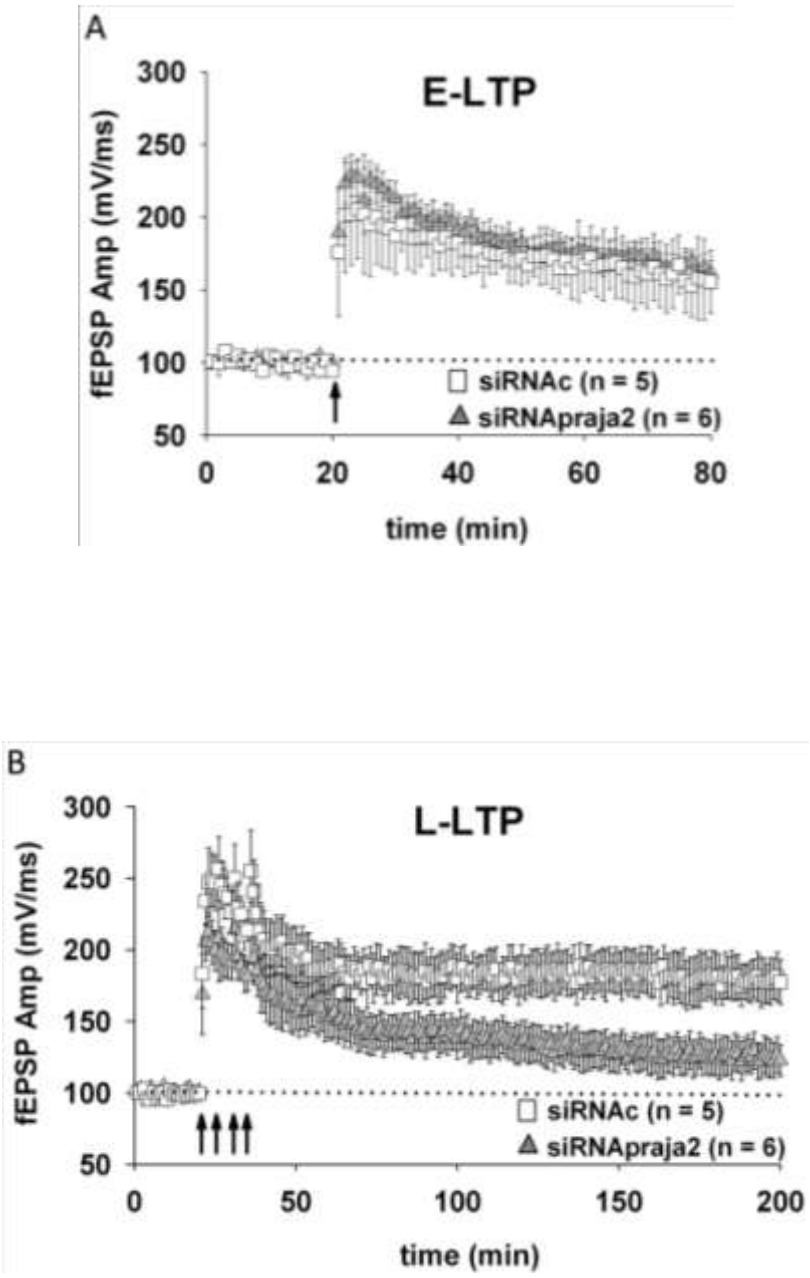

Figure 22. praja2 controls cAMP-dependent L-LTP formation in rat brain. (**A**) The early phase of LTP (E-LTP) induced by one train of HFS is comparable between siRNAc (white squares) and siRNApraja2-rats (grey triangles). fEPSP amplitudes are expressed as percentage of pretetanus baseline. (**B**) Time plot of field excitatory post-synaptic potential (fEPSP) responses for group data, showing that TBS protocol elicits normal LTP in siRNAc-rats (white squares), but deficient LTP in siRNApraja2-rats (grey squares). fEPSP amplitudes are expressed as percentage of pretetanus baseline.

DISCUSSION

Activation of PKA is rapidly followed by a refractory period during which ligand-stimulated cells become less responsive to the next cAMP wave. Phosphodiesterases, Ser/Thr phosphatases and transcriptional regulation of components of the cAMP signaling cascade control the establishment and maintenance of the refractory period *(Houslay et al., 2007; Canettieri et al., 2003; Armstrong et al., 1995).*

The relative abundance of R and PKAc subunits also contributes to the strength and duration of cAMP signalling. For example, increased PKAc activity profoundly alters the sensitivity of cells to ligand stimulation, sustaining downstream cAMP signalling and impacting on different aspects of cellular behaviour *(Davis et al., 1998; Amieux et al., 2002).*

Deletion of the PKA RIIα/β regulatory subunit in mice enhances basal activity of PKAc subunits, leading to increased metabolic rate in adipose tissue and impairment of neuronal activities *(Newhall et al., 2005; Cummings et al., 1996).* In Aplysia sensory neurons, ubiquitin-dependent proteolysis of R subunits facilitates downstream PKAc signalling and controls induction and consolidation of long-term memory *(Chain et al., 1999; Hegde et al., 1993).* However the E3 ubiquitin-ligase controlling the stability of R subunits in eukaryotes was unknown.

We have identified praja2 as the E3 ligase that ubiquitinates and degrades mammalian R subunits. praja2-PKA complexes optimally decode signals generated at cell membranes and rapidly propagate the cAMP input to the downstream effector kinase. Overexpression of praja2 induces proteolysis of R subunits, whereas genetic knock-down of the ligase prevents cAMP-induced decline of R subunits levels. Under basal conditions, praja2 controls the bulk levels of compartmentalized PKA holoenzyme. Elevation of cAMP levels increases praja2-PKA complex formation, favoring efficient and synchronised local activation of the kinase. Phosphorylation of praja2 by PKAc enhances proteolysis of R subunits and reduces the stoichiometric ratio of R/PKAc, sustaining substrate phosphorylation by the activated Kinase. The molecular events controlled by praja2 ultimately impact on the amplitude of PKA signalling (i.e. CREB phosphorylation and nuclear gene transcription) and significantly contribute to synaptic plasticity and long-term memory.

Collectively, our findings indicate that PKA regulated proteolysis of R subunits by praja2 constitutes an important positive feed-back mechanism that controls the rate and magnitude of cAMP-PKA signalling. Understanding the intricate connection between hormone-generated signals and the ubiquitin-proteasome

pathway, and identifying the mechanism(s) underlying cAMP signal generation and attenuation at target sites provides basic insights into hormone action.

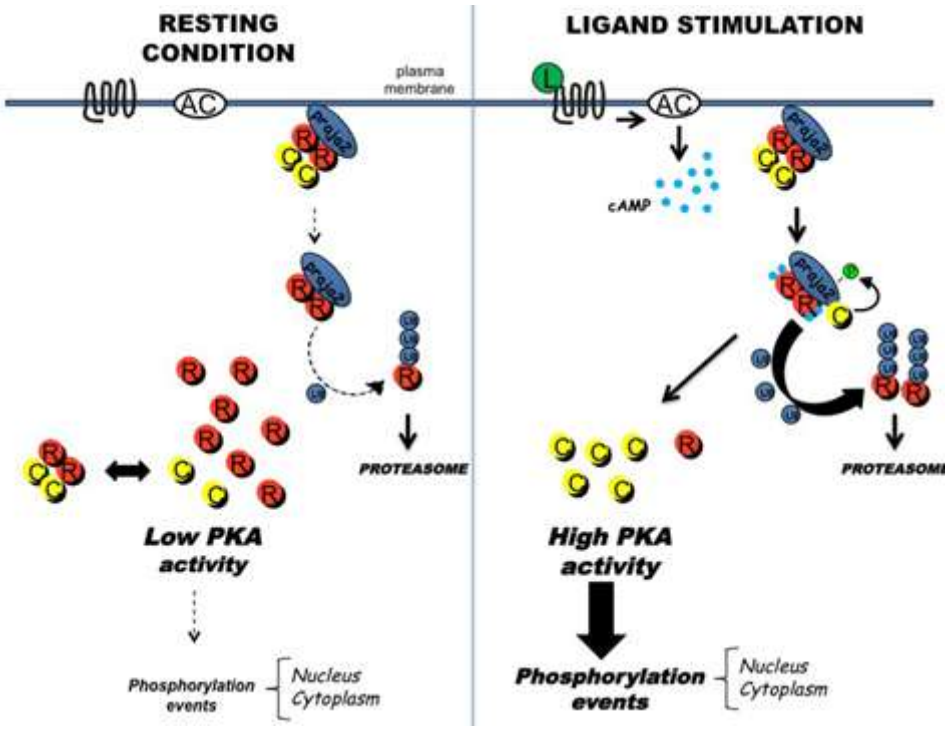

Figure 23. Molecular mechanism model. Under resting conditions, PKA holoenzyme accumulates inside the cells as consequence of low ubiquitination rate of R subunits. Elevation of intracellular cAMP levels by ligand (L) stimulation of the adenylate cyclase (AC) efficiently activates PKA, which in turn phosphorylates praja2. Phosphorylated praja2 ubiquitinates and degrades R subunits through the proteasome pathway. Accumulation of free, active PKAc (C) sustains substrate phosphorylation and positively impacts on the amplitude of cAMP signalling.

METHODS

Cell lines. Human embryonic kidney cell line (HEK293) and neuroblastoma cells (SHSY5Y) were cultured in Dulbecco modified Eagle's medium containing 10% fetal bovine serum in an atmosphere of 5% CO2. Where indicated, cells were propagated in

DMEM medium supplemented with 10% calf serum. Hippocampal neurons were prepared from 18 days old rat embryos. Neurons were cultured at 37°C in a humidified 5% CO2 atmosphere with medium replenishment after 6 days, and used after 11 days of culture in all experiments.

Animals. Female Wistar rats (Charles River) were housed in diurnal lighting conditions (12 hours darkness and 12 hours light) and fasted overnight but allowed free access to water before the experiment. Experiments were performed according to international guidelines for animal research and the experimental protocol was approved by the Animal Care Committee of the University of Naples.

Plasmids and transfection. Vectors encoding the flag-praja2, GFP-praja2 and GSTpraja2 were purchased from Genecopeia. praja2rm was generated by site-directed mutagenesis, while praja2 deletion mutants and GST-fusions were generated by PCR with specific oligonucleotide primers. PCR products were subcloned into the

same vector of wild-type praja2 cDNA. HA-tagged ubiquitin was provided by Dr Antonio Leonardi (University of Naples, Italy); epitope tagged RIα and RIIα/β vectors were provided by Dr Ginsberg SH *(Lim et al., 2007)*. SMART pool siRNAs targeting coding regions and 3'UTR of distinct segments of praja2 and RIIα/β were purchased from Dharmacon and Sigma. The siRNAs were transiently transfected using Lipofectamine 2000 (Invitrogen) at a final concentration of 100 pmol/ml of culture medium.

Antibodies and chemicals. Rabbit polyclonal antibodies directed against RIIβ, RIIα, RIα, PKAc, ERK2, hemaglutinin epitope (HA.11), glutathione S-transferase (GST), CaMKIIα were purchased from SantaCruz; we also used antibodies directed against RIIβ, RIIα, RIα purchased from BD Transduction; α−tubulin, flag and myc epitope from Sigma; phosphoser133-CREB and CREB from Millipore; two distinct polyclonal antibodies directed against human praja2 were generated in rabbit using the following epitopes: 1) residues 480-631; 2) residues 60-250. Both antibodies gave similar immunostaining patterns. Forskolin, isoproterenol and cAMP were purchased from Sigma.

Immunoprecipitation and pull down assay. Cells (or rat tissues) were homogenized in lysis buffer (50mMTris-HCl, pH 7.4, 0.15MNaCl, 100 mM EDTA,0.5% NP40) containing aprotinin (5

μg/ml), leupeptin (10 μg/ml), pepstatin (2 μg/ml), and 0.5 mM phenylmethylsulfonyl fluoride. The lysates were cleared by centrifugation at 15,000 g for 15 min. Cell lysates (2 mg) were immunoprecipitated with the indicated antibodies. An aliquot of cell lysate (100 μg) or immunoprecipitates were resolved by SDS-PAGE gel and transferred to Protran membrane. The immunoblot analysis was performed as previously described. Chemoluminescent (ECL) signals were quantified by scanning densitometry (Molecular Dynamics, Sunnyvale, CA). GST fusions were expressed and purified from BL21 (DE3) pLysS cells. 20 μl of GST or GST-praja2 beads were incubated with 2 mg of cell lysate or with in vitro translated [35S]-labeled R subunits in 200 μl lysis buffer (150 mM NaCl, 50 mM Tris-HCl pH 7.5, 1 mM EDTA, 0.5% triton X-100) in rotation at 4 °C overnight. Pellets were washed four times in lysis buffer supplemented with NaCl (0.4 M final concentration) and eluted in Laemmli buffer. Eluted samples were resolved by 8%-PAGE gel, transferred to polyvinyldene difluoride membranes and immunoblotted with the indicated antibody.

In vitro kinase assay and RII-Overlay Analysis. Flag-tagged praja2 and S342A,T389A mutant transiently expressed in HEK293 cells were immunoprecipitated with anti-flag antibody. The precipitates were washed twice in kinase buffer (10 mM MgCl2, 20mM Hepes,

pH 7.4) and resuspended in the same buffer (50 µl) containing 10 µM ATP, 10 µCi of [γ-32P]ATP (Amersham Corp.), 100 µM cAMP and 10 units of purified PKAc (Sigma). Following incubation at 30 °C for 10 min, samples were washed three times in kinase buffer, resuspended in Laemily buffer and loaded on SDS-PAGE. Phosphorylated proteins were visualized by autoradiography. An aliquot of the samples was immunoblotted with anti-flag antibodies. PKAc activity was fully inhibited by adding a specific PKA inhibitor peptide (PKI, 10 mM) containing a PKA pseudophosphorylation site (Sigma) (data not shown). RII-overlay assay was performed as previously described24, with the exception that RIIβ-binding proteins were visualized by immunoblotting the filter with anti-RIIβ antibody.

In vitro ubiquitination assay. [35S]-labeled R subunits praja2 were synthesized in vitro using TnT quick coupled transcription/translation system (Promega) in the presence of 45

µCi of [35S]-labeled methionine. The ubiquitination assay was performed in buffer containing 50 mM Tri-HCl pH 7.5, 0.6 mM dithiothreitol, 5mM MgCl2, supplemented with recombinant his-ubiquitin (2.5 µg/µl), 2 mM ATP, E1 (1.5 ng/µl) (Affinity Research, Exeter, UK), purified E2 (10 ng/µl) (UbcH5b) in the presence or absence of agarose beads-bound praja2-flag or its mutants

immunoprecipitated from cell lysates. The reaction mixture was incubated at 30oC for 90 min, then stopped with Laemmli buffer and size-fractionated on 8% SDS-PAGE. Ubiquitination products were visualized by autoradiography.

siRNAs administration into the rat brain. All rats, anesthetized with chloral hydrate (400 mg/kg, i.p.), were put on a stereotaxic frame. A 23-g stainless steel guide cannula (Small Parts, Inc, Miami Lakes, FL) was implanted into the right lateral ventricle, the third ventricle using the stereotaxic coordinates of 0.5 mm caudal to bregma, 2 mm lateral and 2.5 mm below the dura. The cannula was fixed to the cranium using dental acrylic and small screws. siRNAs targeting praja2 (10µl from 250µM stock) and control siRNAs (10µl from 250µM stock) were administered three times, 24 hours, 12 hours and 1 hour before isoproterenol stimulation. Rats were sacrificed 30 min or 60 min later. Distinct brain regions (cortex, hippocampus and striatum) from left and right hemisphere were isolated. Brain tissues were used for immunoblot analysis and RNA extraction.

RNA purification and quantitative PCR analysis. Total RNA was extracted with TRIzol reagent according to the manufacturer's protocol (Sigma, St. Louis, MO, USA). Two micrograms of the isolated RNA were reverse-transcribed with the Omniscript RT kit

(Qiagen, Milan, Italy). Optimal reverse-transcriptase reactions were performed in 20 µl volume consisting of 10X buffer, 1 IU of reverse transcriptase, 10 IU of RNase OUT, 2 mM dNTPs, and 1mM random examers at 37°C for 1 h. Real time PCR was performed in

triplicate in 20 µl reaction volumes using the Power SYBER Green PCR Master Mix (Applied Biosystems, Foster City, CA, USA). PCR primers for human c-fos mRNA are the following: forward 5'-CGGGCTTCAACGCAGACTA; reverse 5'-

GGTCCGTGCAGAAGTCCTG, while for rat c-fos mRNA we used the following primers: forward 5'-AGCATGGGCTCCCCTGTCA; reverse 5'- GAGACCAGAGTGGGCTGCA. Primers were used at final concentration of 4 µM. 18S RNA was used as reference. Real time PCR reactions were carried out in a MJ MiniTM Personal Thermal Cycler apparatus (Bio-Rad Laboratories, CA, USA). Melting curves were obtained by increasing the temperature from 60°C to 95°C with a temperature transition rate of 0.5°C/sec. Melting curves of final PCR products were analysed (OpticonMonitor 3 Bio-Rad).

Confocal microscopy and image analysis. Forebrain coronal vibratome sections were subjected to immunostaining with incubated anti-RIIβ, anti-praja2 and anti-CaMKIIα antibodies. Immunofluorescence was visualized using a Zeiss LSM 510 Meta

argon/krypton laser scanning confocal microscope. Four images from each optical section were averaged to improve the signal to noise ratio. A minimum of four sections per brain and four different samples per region were analyzed. Cultured cells transiently transfected with expression vectors were fixed and immunostained with anti-RIIα/β, anti-PKAc, antiflag or anti-praja2 antibodies. Confocal analysis was performed as above.

cAMP precipitation. β2AR HEK293 cells transiently overexpressing praja2 fusion proteins have been treated with indicated stimuli, were lysed and subjected to precipitations with Rp-8-AHA-cAMP agarose resin (Biolog) for two hours. In this assay, binding of R subunits to the resin-coupled cAMP analogue (= PKA inhibitor Rp-cAMP, inhibits holoenzyme dissociation) results in re-association of activated PKAc and R subunits. To test the impact of cAMP on the complex formation of PKA•praja2 we artificially elevated endogenous cAMP levels with forskolin or through activation of the stably expressed beta2-adrenergic receptor (β2AR) by isoproterenol prior to cell lysis. As control we have added excess of cAMP (5mM) to mask the cAMP binding sites in the R subunits for precipitation. Resin associated complexes have been washed at least four times with the lysis buffer (10 mM sodium phosphate pH 7.2, 150 mM NaCl, 0,5% Triton X100 supplemented with

standard protease inhibitors) and eluted with Laemmli sample buffer and subjected to immunoblot analysis.

Electrophysiology. All animal procedures were in compliance with the European Council Directive (86/609/EEC). Parasagittal hippocampal slices (400 μm) from rats treated with siRNAs targeting praja2 and control siRNA were kept submerged at 30 ºC and superfused (2–3 mL/min) with oxygenated (95% O2, 5% CO2) artificial cerebrospinal fluid (ACSF) containing (in mM): 124 NaCl, 2.5 KCl, 1.25 NaH2PO4, 1.3 MgSO4, 2.4 CaCl2, 26 NaHCO3, and 10 glucose. Presynaptic stimulation was applied to the medial perforant pathway of the dentate gyrus using a bipolar insulated tungsten wire electrode, and field excitatory postsynaptic potentials (EPSPs) were recorded at a control test frequency of 0.033 Hz from the middle one-third of the molecular layer of the dentate gyrus with a glass microelectrode. LTP was induced with theta burst stimulation (TBS) consisting of nine bursts of four pulses at 100 Hz, 200 ms interburst interval, 5 min intertrain interval. All solutions contained 100 μM picrotoxin (Sigma) to block GABAA-mediated activity.

All data are presented as mean ± SEM and “n” indicates the number of slices. Statistical significance was evaluated by unpaired Student's t test. Statistical significance was set at $p < 0.05$.

REFERENCES

- **Adams M. R., Brandon E. P., Chartoff, E. H. Idzerda, R. L. Dorsa, D. M. & McKnight, G. S. (1997).** Loss of haloperidol induced gene expression and catalepsy in protein kinase A-deficient mice. Proc. Natl Acad. Sci. USA, 94, 12157-12161.

- **Amieux PS, Howe DG, Knickerbocker H, Lee DC, Su T, Laszlo GS, Idzerda RL, McKnight GS.** Increased basal cAMP-dependent protein kinase activity inhibits the formation of mesoderm-derived structures in the developing mouse embryo. J Biol Chem 277, 27294-304 (2002).

- **Armstrong R., Wen W., Meinkoth J., Taylor S. & Montminy, M.** A refractory phase in cyclic AMP-responsive transcription requires down regulation of protein kinase A. Mol Cell Biol 15, 1826-32 (1995).

- **Beene D. L. & Scott J. D.** A-kinase anchoring proteins take shape. Curr Opin Cell Biol 19, 192-8 (2007).

- **Brandon E. P., Idzerda R. L. & McKnight G. S.** (1995a). Targeting the mouse genome: a compendium of knockouts. Curr. Biol. 5, 873-881.

- **Brandon E. P., Logue S. F., Adams M. R., Qi M., Sullivan S. P., Matsumoto A. M., Dorsa D. M., Wehner J. M., McKnight G. S. & Idzerda R. L.** (1998). Defective motor behavior and neural gene expression in RIIbeta-protein kinase A mutant mice. J. Neurosci. 18, 3639-3649.

- **Brandon E. P., Zhuo M., Huang Y. Y., Qi M., Gerhold K. A., Burton K. A., Kandel E. R., McKnight G. S. & Idzerda R. L.** (1995b). Hippocampal long-term depression and depotentiation are defective in mice carrying a targeted disruption of the gene encoding the RI beta subunit of cAMP-dependent protein kinase. Proc. Natl Acad. Sci. USA, 92, 8851-8855.

- **Bregman D. B., Hirsch A. H. & Rubin C. S.** Molecular characterization of bovine brain P75, a high affinity binding protein for the regulatory subunit of cAMP-dependent protein kinase II beta. J Biol Chem 266, 7207-13 (1991).

- **Burton K. A., Johnson B. D., Hausken Z. E., Westenbroek R. E., Idzerda R. L., Scheuer T., Scott J. D., Catterall W. A. & McKnight, G. S.** (1997). Type II regulatory subunits are not required for the anchoring-dependent modulation of Ca2. channel activity by cAMP-dependent protein kinase. Proc. Natl Acad. Sci. USA, 94, 11067-11072.

- **Burton, K. A., Treash-Osio, B., Muller, C. H., Dunphy, E. L. & McKnight, G. S.** (1999). Deletion of type II alpha regulatory subunit delocalizes protein kinase A in mouse sperm without affecting motility or fertilization. J. Biol. Chem. 274, 24131-24136.

- **Canettieri G., Morantte I., Guzmán E., Asahara H., Herzig S., Anderson SD., Yates JR 3rd, Montminy M.** Attenuation of a phosphorylation-dependent activator by an HDAC-PP1 complex. Nat Struct Biol 10, 175-81 (2003).

- **Carr D. W., Stofko-Hahn R. E., Fraser I. D., Bishop S. M., Acott T. S., Brennan R. G. & Scott J. D.** (1991). Interaction of the regulatory subunit (RII) of cAMP-dependent protein kinase with RII-anchoring proteins occurs through an amphipathic helix binding motif. J. Biol. Chem. 266, 14188-14192.

- **Cassano S., Di Lieto A., Cerillo R. & Avvedimento E. V.** (1999). Membrane-bound cAMP-dependent protein kinase controls cAMP-induced differentiation in PC12 cells. J. Biol. Chem. 274, 32574-32579.

- **Chain DG., Casadio A., Schacher S., Hegde AN., Valbrun M., Yamamoto N., Goldberg AL., Bartsch D., Kandel ER., Schwartz JH.** Mechanisms for generating the autonomous cAMP-dependent protein kinase required for long-term facilitation in Aplysia. Neuron 22, 147-56 (1999a).

- **Chain D. G., Hegde A. N., Yamamoto N., Liu-Marsh B. & Schwartz J. H.** Persistent activation of cAMP-dependent protein kinase by regulated proteolysis suggests a neuron-specific function of the ubiquitin system in Aplysia. J Neurosci 15, 7592- 603 (1995).

- **Chain D. G., Schwart, J. H. & Hegde A. N.** Ubiquitin-mediated proteolysis in learning and memory. Mol Neurobiol 20, 125-42 (1999b).

- **Chen Y., Cann M. J., Litvin T. N., Iourgenko V., Sinclair M. L., Levin L. R., and Buck J.** (2000) Soluble adenylyl cyclase as an evolutionarily conserved bicarbonate sensor. Science 289, 625.628.

- **Ciechanover A.** (1998) The ubiquitin-proteasome pathway: on protein death and cell life.EMBO J. 17 (24), 7151–7160.

- **Cummings D. E., Brandon E. P., Planas J. V., Motamed K., Idzerda R. L. & McKnight G. S.** (1996). Genetically lean mice result from targeted disruption of the RII beta subunit of protein kinase Nature, 382, 622-626.

- **Davis G. W., Di Antonio A., Petersen S. A. & Goodman C. S.** Postsynaptic PKA controls quantal size and reveals a retrograde signal that regulates presynaptic transmitter release in Drosophila. Neuron 20, 305-15 (1998).

- **Dodge K. & Scott J. D.** (2000). AKAP79 and the evolution of the AKAP model. FEBS Letters, 476, 58-61.

- **Edelman A. M., Blumenthal D. K. & Krebs E. G.** (1987). Protein serine/threonine kinases. Annu. Rev. Biochem. 56, 567-613.

- **Edwards A. S. & Scott J. D.** (2000). A-kinase anchoring proteins: protein kinase A and beyond. Curr. Opin. Cell Biol. 12, 217-221.

- **Feliciello A., Gallo A., Mele E., Porcellini A., Troncone G., Garbi C., Gottesman M. E. & Avvedimento E. V.** (2000). The localization and activity of cAMP-dependent protein kinase affect cell-cycle progression in thyroid cells. J. Biol. Chem. 275, 303-311.

- **Feliciello A., Giuliano P., Porcellini A., Garbi C., Obici S., Mele E., Angotti E., Grieco D., Amabile G., Cassano S., Li Y., Musti A. M.,**

Rubin C. S., Gottesman M. E. & Avvedimento E. V. (1996). The v-Ki-Ras oncogene alters cAMP nuclear signaling by regulating the location and the expression of cAMP-dependent protein kinase II beta. J. Biol. Chem. 271, 25350-25359.

- **Feliciello A., Gottesman M. E. & Avvedimento E. V.** The biological functions of A-kinase anchor proteins. J Mol Biol 308, 99-114 (2001).

- **Feliciello A., Li Y., Avvedimento E. V., Gottesman M. E. & Rubin C. S**. A-kinase anchor protein 75 increases the rate and magnitude of cAMP signaling to the nucleus. Curr Biol 7, 1011-4 (1997).

- **Feliciello A., Rubin C. S., Avvedimento V. E. & Gottesman M. E.** (1998). Expression of A kinase anchor protein121 is regulated by hormones in thyroid and testicular germ-cells. J. Biol. Chem. 273, 23361-23366.

- **Fimia GM, Sassone-Corsi P** (2000). Cyclic AMP signalling.J Cell Sci. 2001 Jun;114(Pt11):1971-2.

- **Freemont PS (1993).** The RING finger: a novel protein sequence motif related to the zinc finger. Ann NY Acad Sci 684: 174-192.

- **Hausken Z. E., Coghlan V. M., Hastings C. A., Reimann E. M. & Scott J. D.** (1994). Type II regulatory subunit (RII) of the cAMP-dependent protein kinase interaction with A-kinase anchor proteins requires isoleucines 3 and 5. J. Biol. Chem. 269, 24245-24251.

- **Hausken Z. E., Dell'Acqua M. L., Coghlan V. M. & Scott J. D.** (1996). Mutational analysis of the A kinase anchoring protein (AKAP)-binding site on RII. Classification of side-chain determinants for anchoring and isoform selective association with AKAPs. J. Biol. Chem. 271, 29016-29022.

- **Hegde AN., Inokuchi K., Pei W., Casadio A., Ghirardi M., Chain DG., Martin KC., Kandel ER., Schwartz JH.** Ubiquitin C-terminal

hydrolase is an immediate-early gene essential for long-term facilitation in Aplysia. Cell 89, 115-26 (1997).

- **Hegde AN., Goldberg A. L. & Schwartz J. H**. Regulatory subunits of cAMP-dependent protein kinases are degraded after conjugation to ubiquitin: a molecular mechanism underlying long-term synaptic plasticity. Proc Natl Acad Sci U S A 90, 7436-40 (1993).

- **Hershko A., and Ciechanover A.** (1998) The ubiquitin system. Annu Rev Biochem. 1998;67:425-79. Review.

- **Houslay M.D., Baillie G. S. & Maurice D. H.** cAMP-Specific phosphodiesterase-4 enzymes in the cardiovascular system: a molecular toolbox for generating compartmentalized cAMP signaling. Circ Res 100, 950-66 (2007).

- **Houslay M.D. and Adams D.R.** (2003) PDE4 cAMP phosphodiesterases: modular enzymes that orchestrate signalling cross-talk, desensitization and compartmentalization. Biochem. J. 370, 1–18.

- **Huang L. J., Durick K., Weiner J. A., Chun J. & Taylor S. S.** (1997a). Identification of a novel protein kinase A anchoring protein that binds both type I and type II regulatory subunits. J. Biol. Chem. 272, 8057-8064.

- **Huang Y. Y. & Kandel E. R**. Recruitment of long-lasting and protein kinase A-dependent long-term potentiation in the CA1 region of hippocampus requires repeated tetanization. Learn Mem 1, 74-82 (1994).

- **Joazeiro C.A., and Weissman A.M.** (2000) RING finger proteins: mediators of ubiquitin ligase activity. Cell. Sep 1;102(5):549-52. Review.

- **Kitada T., Asakawa S., Hattori N., Matsumine H., Yamamura Y., Minoshima S., Yokochi M., Mizuno Y., Shimizu N.** (1998).

Mutations in the parkin gene cause autosomal recessive juvenile parkinsonism. Nature 392: 605–608.

- **Lester L. B., Langeberg L. K. & Scott J. D.** (1997). Anchoring of protein kinase A facilitates hormone mediated insulin secretion. Proc. Natl Acad. Sci. USA, 94, 14942-14947.

- **Li Y. & Rubin C. S.** (1995). Mutagenesis of the regulatory subunit (RII beta) of cAMP-dependent protein kinase II beta reveals hydrophobic amino acids that are essential for RII beta dimerization and/or anchoring RII beta to the cytoskeleton. J. Biol. Chem. 270, 1935-1944.

- **Lim CJ., Han J., Yousefi N., Ma Y., Amieux PS., McKnight GS., Taylor SS., Ginsberg MH.** Alpha4 integrins are type I cAMP-dependent protein kinase-anchoring proteins. Nat Cell Biol 9, 415-21 (2007).

- **Lonze B. E. & Ginty D. D**. Function and regulation of CREB family transcription factors in the nervous system. Neuron 35, 605-23 (2002).

- **Lorick K.L., Jensen J.P., Fang S., Ong A.M., Hatakeyama S. and Weissman A.M.** (1999) RING fingers mediate ubiquitin-conjugating enzyme (E2)-dependent ubiquitination. Proc Natl Acad Sci U S A. Sep 28;96(20):11364-9.

- **Qi M., Zhuo M., Skalhegg B. S., Brandon E. P., Kandel E. R., McKnight G. S. & Idzerda R. L.** (1996). Impaired hippocampal plasticity in mice lacking the C beta1 catalytic subunit of cAMP dependent protein kinase. Proc. Natl Acad. Sci. USA, 93, 1571-1576.

- **Malleret G., Alarcon JM., Martel G., Takizawa S., Vronskaya S., Yin D., Chen IZ., Kandel ER., Shumyatsky GP**. (2010). Bidirectional regulation of hippocampal longterm synaptic plasticity and its influence on opposing forms of memory. J Neurosci 30, 3813-25.

- **Mattsson K., Pokrovskaja K., Kiss C., Klein G., and Szekely L.** (2001). Proteins associated with the promyelocytic leukemia gene

product (PML)-containing nuclear body move to the nucleolus upon inhibition of proteasome-dependent protein degradation. Proc. Natl. Acad. Sci. USA 98: 1012–1017.

- **McKnight G. S., Cummings D. E., Amieux P. S., Sikorski M. A., Brandon E. P., Planas J. V., Motamed K. & Idzerda R. L.** (1998). Cyclic AMP, PKA, and the physiological regulation of adiposity. Recent Prog. Horm. Res. 53, 139-159.

- **Meinkoth J. L., Alberts A. S., Went W., Fantozzi D., Taylor S. S., Hagiwara M., Montminy M. & Feramisco J. R.** (1993). Signal transduction through the cAMP-dependent protein kinase. Mol. Cell. Biochem. 127-128, 179-186.

- **Montminy M.** (1997). Transcriptional regulation by cyclic AMP. Annu. Rev. Biochem. 66, 807-822.

- **Nakayama M., Miyake T., Gahara Y., Ohara O., and Kitamura T.** (1995). A novel RING-H2 motif protein downregulated by axotomy: its characteristic localization at the postsynaptic density of axosomatic synapse. J. Neurosci. 15: 5238–5248.

- **Newhall K. J., Cummings D. E., Nolan M. A. & McKnight G. S.** Deletion of the RIIbeta-subunit of protein kinase A decreases body weight and increases energy expenditure in the obese, leptin-deficient ob/ob mouse. Mol Endocrinol 19, 982-91 (2005).

- **Newlon M.G., Roy M., Hausken ZE., Scott JD., Jennings JA.** (1999) The A-kinase anchoring domain of type IIa cAMP-dependent protein kinase is highly helical. J. Biol. Chem. 272, 23637–23644.

- **Ohara 0., Teraoka H.** (1987). Anomalous behavior of human leukocvte interferon subtypes on polyacrylamide gel electrophoresis in the presence of dodecyl sulfate. FEBS Lett 211:78-82.

- **Paolillo M., Feliciello A., Porcellini A., Garbi C., Bifulco M., Schinelli S., Ventra C., Stabile E., Ricciardelli G., Schettini G. & Avvedimento E. V.** (1999). The type and the localization of

cAMPdependent protein kinase regulate transmission of cAMP signals to the nucleus in cortical and cerebellar granule cells. J. Biol. Chem. 274, 6546-6552.

- **Ping Yu, Yiwang Chen, Danilo A. Tagle, and Tao Cai** (2002) PJA1, Encoding a RING-H2 Finger Ubiquitin Ligase, Is a Novel Human X Chromosome Gene Abundantly Expressed in Brain. Genomics. 79, 869-874.

- **Rubin C. S.** 1994. A kinase anchor proteins and the intracellular targeting of signals carried by cyclic AMP. Biochim. Biophys. Acta 1224:467–479.

- **Rubino H. M., Dammerman M., Shafit-Zagardo B. & Erlichman, J**. Localization and characterization of the binding site for the regulatory subunit of type II cAMP-dependent protein kinase on MAP2. Neuron 3, 631-8 (1989).

- **Siderius LE, Hamel BC, van Bokhoven H, de Jager F, van den Helm B, Kremer H, Heineman-de Boer JA, Ropers HH, Mariman EC** (1999). X-linked mental retardation associated with cleft lip/palate maps to Xp11.3- 21.3. Am. J. Med. Genet. 85: 216–220.

- **Stein J. C., Farooq M., Norton W. T. & Rubin C. S.** (1987) Differential expression of isoforms of the regulatory subunit of type II cAMP-dependent protein kinase in rat neurons, astrocytes, and oligodendrocytes J. Biol. Chem. 262, 3002-3006.

- **Stork O., Stork S., Pape H. C., and Obata K.** (2001). Identification of genes expressed in the amygdala during the formation of fear memory. Learn. Mem. 8: 209– 19.

- **Su Y., Dostmann WRG., Herberg FW., Durick K., Xuong N-H., Ten Eyck L, Taylor SS., Varughese KI** (1995). Regulatory subunit of protein kinase A: structure of deletion mutant with cAMP binding domains. Science 269:807–813.

- **Sutherland EW** (1970). On the biological role of cyclic AMP.JAMA. 1970 Nov 16;214(7):1281-8. Review.

- **Tasken K. and Aandahl E. M**. Localized effects of cAMP mediated by distinct routes of protein kinase A. Physiol Rev 84, 137-67 (2004).

- **Taylor S. S., Knighton D. R., Zheng J., Ten Eyck L. F. & Sowadski J. M.** (1992). Structural framework for the protein kinase family. Annu. Rev. Cell Biol. 8, 429-462.

- **Tunquist BJ., Hoshi N., Guire ES., Zhang F., Mullendorff K., Langeberg LK., Raber J., Scott JD.** Loss of AKAP150 perturbs distinct neuronal processes in mice. Proc Natl Acad Sci U S A 105, 12557-62 (2008).

- **Wang Y., Scott JD., McKnight GS., Krebs EG**. (1991) A constitutively active holoenzyme from the cAMP-dependent protein kinase. Proc Natl Acad Sci U S A 88:2446–2450.

- **Wang L., Sunahara RK., Krumins A., Perkins G., Crochiere ML., Mackey M. Bell S., Ellisman MH., Taylor SS**. (2001) Cloning and mitochondrial localization of full length D-AKAP2, a protein kinase A anchoring protein. Proc. Natl. Acad. Sci. U. S. A. 98, 3220–3225.

- **Wilson M., Mulley J., Gedeon A., Robinson H., and Turner G.** (1991). New X-linked syndrome of mental retardation, gynecomastia, and obesity is linked to DXS255. Am. J. Med. Genet. 40: 406–413.

- **Yu P., Chen Y., Tagle D. A. & Cai T**. PJA1, encoding a RING H2 finger ubiquitin ligase, is a novel human X chromosome gene abundantly expressed in brain. Genomics 79, 869-74 (2002).

- **Zhong H, Sia GM, Sato TR, Gray NW, Mao T, Khuchua Z, Huganir RL, Svoboda K.** Subcellular dynamics of type II PKA in neurons. Neuron 62, 363-74 (2009).

- **Zhou Y, Takahashi E, Li W, Halt A, Wiltgen B, Ehninger D, Li GD, Hell JW, Kennedy MB, Silva AJ.** Interactions between the NR2B receptor and CaMKII modulate synaptic plasticity and spatial learning. J Neurosci 27, 13843-53 (2007).

- **Zippin JH., Chen Y., Nahirney P., Kamenetsky M., Wuttke MS., Fischman DA., Levin LR., and Buck J.** (2003) Compartmentalization of bicarbonate-sensitive adenylyl cyclase in distinct signaling microdomains FASEB J. Jan;17(1):82-4.